A THESIS REPORT ON

FACILE SYNTHESIS OF rGO/Ag NANOCOMPOSITES FOR THE DETECTION OF CHEMICALS AND ANTIBACTERIAL ACTION

THESIS SUBMITTED TO
MAHATMA GANDHI UNIVERSITY

In partial fulfilment of the requirements for the award of the degree in
MASTER OF PHILOSOPHY IN PHYSICS

BY

ANJALY T R
REG NO: SMP20PHY002

UNDER THE SUPERVISION OF

Dr. PRIYA PARVATHI AMEENA JOSE
Head of the Department
Department of Physics
ST. TERESA'S COLLEGE (AUTONOMOUS), ERNAKULAM
Cochin-682011

Department of Physics
ST. TERESA'S COLLEGE (AUTONOMOUS), ERNAKULAM
Cochin-682011

(AFFILIATED TO MAHATMA GANDHI UNIVERSITY, KOTTAYAM)
2020-2021

ST. TERESA'S COLLEGE (AUTONOMOUS)

ERNAKULAM

(Affiliated to Mahatma Gandhi university, Kottayam)

DEPARTMENT OF PHYSICS

THESIS REPORT

2020-2021

CERTIFICATE

This is to certify that the thesis report titled "**FACILE SYNTHESIS OF rGO/Ag NANOCOMPOSITES FOR THE DETECTION OF CHEMICALS AND ANTIBACTERIAL ACTION"** is the bonafide record of the project work done by **ANJALY T R**, REG NO: **SMP20PHY002**, a student of the department of Physics M.Phil. Physics, St. Teresa's college, Ernakulam during the academic year 2020-2021, in partial fulfilment of the requirement for the Degree of Master of Philosophy in Physics, Mahatma Gandhi University, Kottayam, Kerala.

Place: Ernakulam

Date:

Dr. Priya Parvathi Ameena Jose
(Supervising Guide)
Department of Physics
St. Teresa's college, Ernakualm

Valued by Examiners

1.

FACILE SYNTHESIS OF rGO/Ag NANOCOMPOSITES FOR THE DETECTION OF CHEMICALS AND ANTIBACTERIAL ACTION

M.Phil. THESIS

AUTHOR

ANJALY T R

Department of Physics

St. Teresa's college, Ernakulam

Cochin- 682011

SUPERVISOR

Dr. PRIYA PARVATHI AMEENA JOSE

Head of the Department
Department of Physics
ST. TERESA'S COLLEGE (AUTONOMOUS), ERNAKULAM
Cochin-682011

2020-2021

PAPER PRESENTATIONS

1. **"International Online Conference on Nano Materials (ICN 2022)",** jointly organized by **International and Interuniversity Centre for Nanoscience and Nanotechnology (IIUCNN), School of Energy Materials (SEM), Mahatma Gandhi University, Kottayam, Kerala, India, University of Johannesburg, Doornfontein, Johannesburg, South Africa, Wroclaw University of Technology, Poland, Gdansk University of Technology, Poland, University of Lorraine, Nancy, France,** under the title **"rGO/Ag nanocomposites as an efficient SERS substrate for the detection of chemicals".**

2. **National Seminar on "Substantial Innovations in Functional Materials: Developments and Applications",** jointly organized by **Science Departments, Al-Ameen College, Edathala and The Indian Science Congress Association- Cochin Chapter (ISCA)** under the title **"Synthesis and characterisation of rGO/Ag nanocomposites for SERS application".**

3. **"Annual Physics Symposium (APS) 2022",** organized by **Department of Physics & Centre for Research, St. Teresa's College, (Autonomous), Ernakulam** under the title **"Synthesis & characterisation of GO/Ag nanocomposites with SERS activity for their application in pesticide detection".**

DECLARATION

I **ANJALY T R**, Master of Philosophy in Physics, Department of Physics and Centre for Research, St. Teresa's college, Ernakulam do here by declare that this project work titled "**FACILE SYNTHESIS OF rGO/Ag NANOCOMPOSITES FOR THE DETECTION OF CHEMICALS AND ANTIBACTERIAL ACTION" submitted to Mahatma Gandhi University,** Kottayam in partial fulfilment of the requirements for the award of the degree of Master of Philosophy in Physics is a record of original work done by me under the supervision of Dr. Priya Parvathi Ameena Jose, Head of the Department, Department of Physics, St. Teresa's college, Ernakulam and is not previously formed the basis for award of any degree or diploma of other similar title to any candidate of this or any other university.

ANJALY T R

Place: Ernakulam
Date:

ACKNOWLEDGEMENTS

I have great pleasure in extending my whole hearted thanks to all the people who helped me directly and indirectly in this endeavour. First and foremost, I praise God Almighty, for enabling me to complete the project in time and its fullness.

With great happiness, I express my sincere gratitude to my project supervisor, Dr. Priya Parvathi Ameena Jose, Head of the Department, Department of Physics, St. Teresa's college, Ernakulam, for her guidance, suggestions and continuous encouragement offered to me throughout the course of this project.

I am extremely thankful to Associate Prof. Vimala George, Department of Physcis, St. Xavier's college, Aluva, Ernakulam, for her co – guidance and valuable help. I also put forward my sincere thanks to Dr. Lizzy Mathew, the former Principal and Dr. Alphonsa Vijaya Joseph, the principal of St. Teresa's college, Ernakulam, for providing permission and encouragement to carry out this work.

I express my profound sense of thankfulness to Dr. Susnsu Kuriyan Thottil and Dr. Anju K Nair, Faculty at St. Teresa's college, Department of Physics, for their help and valuable suggestions during my project work.

I would like to express my sinciere thanks to Department of Chemistry, st. Teresa's college, Ernakulam, for their help during my entire work.

I am also indebted to Mrs. Glaxy and all the research scholars at the Department of Botany, for their immense help during my project work.

I would like to express my gratitude towards Sophisticated Test & Instrumentation Centre (STIC), CUSAT, EMF-SAIF Kottayam and Department of Optoelectronics, University of Kerala, Thiruvananthapuram for extending their services in the analysis section. This project would not be complete without the analysis results obtained from these centres.

I am also grateful towards all the members of faculty and my colleges Anakha M, Sr. Achal Grace, Farsana K S, Merly Ann Peter and Rajani R Nair at St. Teresa's college, Department of Physics and Centre for Research, for their love, encouragement, patience and support, without which this project wouldn't be a success.

Now I would like to pay high regards to three very special persons in my life, my parents and my brother for their unconditional love, encouragement, patience and support throughout my life and lifting me uphill this phase of life. I owe everything to them and I know this would not have been a reality without their love and support.

With pleasure I would like to express my sincere gratitude towards Mr. Hari Sanker G, Faculty member and Research scholar at Department of Physics, Amrita Vishwa Vidyapeetham, Amritapuri campus, Kollam, who were always there with a hand of help in all difficulties towards fulfilling this project.

Anjaly T R

PREFACE

Nano technology is the branch of science that deals with the matter of small dimensions. Their introduction leads to drastic change in the existing discoveries. Generally, when materials reduced to the nano dimension, they process different properties than the bulk. The mechanical properties, electrical properties, optical properties etc. are increases as we go down to the nano dimensions. Each nano structure shows unique properties depending upon the synthesis methods they follow. When materials are made into hybrid with other materials, it enhances the different properties of the whole system.

Among noble metals, silver has gained huge attention due to its tunable properties and wide range of applications. It is considered as superior than any other metal structures. The silver nano structure has gained attention due to its size and its applications in transparent conductive films, antibacterial activity, catalytic applications etc. The integration of metal nano particles on the suitable support stand can improve its efficiency by removing the agglomeration and coalescence of NPs. Here graphene oxide support is chosen due to their adsorption ability and the presence of more active sites.

This work is focused on the surface enhanced Raman scattering (SERS) application of reduced Graphene oxide/ Silver (rGO/Ag) nano composites and to study their antibacterial action. The thesis entitled “FACILE SYNTHESIS OF rGO/Ag NANOCOMPOSITES FOR THE DETECTION OF CHEMICALS AND ANTIBACTERIAL ACTION” is divided into six chapters.

Chapter 1deals with the introductory concepts of nano science and nano technology. An account on silver nano particles and their incorporation on graphene oxide sheet with their application are also added.

Chapter 2 describes the general synthesis methods of graphene oxide including synthetic and free-water oxidation methods. Physical, chemical, photochemical, biological method of synthesis of Silver nano particles are also included in this chapter.

Chapter 3 describes the general characterization techniques used for the analysis of graphene oxide nano particles and the reduced graphene oxide/ silver nano composites.

Chapter 4 consists of the preparation method and characterization tools employed in the structural, morphological and optical analysis of as prepared samples of graphene oxide nanosheets and the reduced graphene oxide/ silver nano composites.

Chapter 5 deals with the Surface enhanced Raman scattering (SERS) applications of reduced graphene oxide/ silver nano composites as a dye/pesticide detector and as an antibacterial agent.

Chapter 6 includes the general conclusions drawn from the studies and the future scope of the work.

CONTENTS

CHAPTER 1

INTRODUCTION

CHAPTER 2

GENERAL SYNTHESIS METHODS

CHAPTER 3

CHARACTERIZATION TECHNIQUES

List of Figures

CHAPTER 1

CHAPTER 2

CHAPTER 3

CHAPTER 4

CHPATER 5

CHAPTER 1

INTRODUCTION

When it comes to the basic requirements for human survival, food, clothing and shelter have always remained to be our top priority throughout history. The ever-increasing population levels has sustained a rocketing demand in food production and with it the use of pesticides have also increased considerably. According to the latest data by FAO, around 58160 tonnes of pesticides of thousands of varieties were utilized in 2018 [1]. Whereas a dauntingly large number of studies have shown that the over dosage of these pesticides including insecticides, fungicides and herbicides end up polluting the environment and ecology. And this which in turn imposes a threat to human health [2-4]. Despite regulations many banned chemicals are still in use all over the world. It is high time that we detect and monitor the usage of such chemicals even at low concentrations. However, the quest for an ultimate solution still remains unanswered. Analytical methods like gas chromatography- mass spectroscopy (GC-MS), liquid chromatography mass spectroscopy (LC-MS), high performance liquid chromatography (HPLC), etc., have been employed for pesticide detection in the past, however, they have all been met with some or the other limitations [5][6][7]. These methods are highly time consuming and require well-equipped laboratories and sample pre- treatments leading to them being replaced by some simpler, faster, reliable and effective methods for the quantitative detection of chemicals simultaneously [8][9][10].

It is reported that a simple and non-destructive technique- Raman scattering called as Surface enhanced Raman scattering (SERS) can partly remedy the limitations mentioned above [11-13]. Since the SERS spectra can provide 'finger print like' information about a particular analyte, it can be used as a sensitive technique for the on-site detection of trace amount of pesticides and other chemicals [14].

There are two mechanisms electromagnetic enhancement (EM) and chemical enhancement (CM) that usually contribute to the SERS enhancement, of which the major player is electromagnetic enhancement. This relies on enhancement of the local electromagnetic field produced by the amplification of the light by the excitation of localized surface plasmon resonances (LSPRs). Chemical enhancement emerges from the modifications of external environment and is explained via the charge-transfer mechanism between the adsorbed molecules and metal surface [15].

As electromagnetic enhancement is the major contributor, most of the studies are oriented towards synthesizing SERS substrates with nano sized plasmonic structures of noble metals like gold and silver due to the location of their SPR bands in the visible and near infrared range. Another development is in terms of successfully fabricating reliable graphene based SERS substrates which contributes to strong chemical enhancement [16].

The prefix 'nano' means 'dwarf' in Greek. One billionth of a meter or one thousand millionth of a meter or 10^{-9} m is called a nano meter (nm). In other words, ten hydrogen or five silicon atoms aligned in a line can give you a nano meter. Typically, a nano meter range is quite smaller than the micro meter and the material properties will show a drastic change from those at micro meter range. The material properties are varied from bulk to nano size. However, the particle at micro meter will have almost similar properties as that of bulk. Most of the analysis detailed that particles at nano scale have enhanced material properties when compared to the micro meter sized materials as well as the bulk materials. The size of nano particles ranges from sub-nano meter to several hundred nanometers [17]. This field of science is now represented as a milestone in almost all branches of science including physics, chemistry, botany, zoology, computer science, medicine, and even in the field of engineering. The study that deals with the maneuvering of small sized materials; that is, at atomic and molecular scales is called as 'nanoscience' and the study that deals with the fabrication, assembling and commercialization of these small structures is called nanotechnology.

Its introduction led to drastic changes in the existing discoveries. Many unknown factors, the wonders that are visible in the nature are well explained from the perspective of nano structures. Why does the peacock feathers appear colourful? How do dolphins communicate under certain level in the sea? How did the lotus leaf get the ability to self-clean? How does the Gecko walk on the wall against gravity? These were some of the questions which remained unanswered before the emergence of nano science. These questions are well explained using the nano structure present in its composition [18][19]. The anti-reflectiveness of moth's eye, the fluid-drag reduction of shark- skin surfaces, etc. are also the examples that gained popularity in the last decade because of the discovery of nano science.

Nano materials have extremely high surface to volume ratios and large surface energy. These makes them more active in reactions than in the bulk state. In addition to those properties there is an effect called "quantum confinement" which is observed when the particle size is reduced much smaller than the wavelength of the electron. Another factor that gets affected by

the cluster size is bandgap. In case of bulk materials, the electrons are not confined. When these particle size gets squeezed into a dimension that of exciton Bohr radius (exciton Bohr radius can be referred to the characteristic radius of electron mobility), they possess higher energy electrons. The confinement of these excitons in one or more dimensions within the material can show fascinating properties. When the size of particle is reduced to nano meter scale, there will be a remarkable change in their mechanical properties, electrical properties, optical properties, chemical properties, thermal properties, magnetic properties, acoustic properties, and so on. In short, one can say that the material properties of metals, semiconductors and insulators are clearly dependent upon the particle size. The classification of materials at nano scale can be done based on differences in dimensions, structures, morphology and so on.

1.1 Classification based on the dimensionality of nano materials

Based on their structure the nano materials can be classified into four main groups as follows:

1.1.1 Zero dimensional

1.1.2 One dimensional

1.1.3 Two dimensional

1.1.4 Three dimensional

1.1.1 Zero dimensional nano structure (Quantum dots):

In zero dimensional (0D) nano structure, all dimensions of that particular structure are in the nano scale, none of the dimensions are in the macro scale. In 0D nano structures, the electrons are confined in three directions. Quantum dots, fullerenes, nano spheres are some examples of 0D nano structures. The size of these particles is on the order of just a few nano meters. Because of their nano metred size, they show unique properties [20].

1.1.2 One dimensional nano structure (Quantum wires):

In 1D nano structures, the electrons are confined in two directions. In these structures, only one dimension is in the macro range, while the rest are in the nano range. Quantum tubes, rods, wires are some examples of these nano structures. The particles having this structure can be used in some applications where tunnelling transport is required [20].

1.1.3 Two dimensional nano structures (Quantum well):

In two dimensional (2D) nano structures, two dimensions are in the macro range. In these nano structures the electrons are confined only in one direction, i.e., electrons can move in the other two directions. They are hence called two dimensional structures. Thin films, plates, sheets, layered structures, all these come under 2D nano structures. There is a particular kind of heterostructures in which a thin "well" layer is sandwiched by two barrier layers. The layer in which both electrons and holes are confined correspond to the perpendicular standing waves in the layers.

1.1.4 Three dimensional structure:

The three dimensional structures are generally called as bulk systems. In this case, there is no restriction to the regular flow of electrons. In other words, the motion is not confined at all. Hence the electrical conduction is easy through them.

1.2 Properties of nano materials

As mentioned earlier, when the material is converted to nano scale from the bulk, there occurs drastic changes in their properties.

1.2.1 Mechanical Properties:

The mechanical properties of the nanomaterials including the hardness, elastic modulus, fracture toughness, scratch resistance and the fatigue strength etc. are different from that of bulk materials when the size is reduced. Along with the size, the internal structural imperfections such as dislocations, micro twins and impurity precipitations are also reduced, thereby it enhances the mechanical properties by lowering the cause of mechanical failure.

The internal imperfections in the nano dimension are highly energetic and will migrate to the surface to relax themselves under annealing, purifying the material and leaving perfect material structures inside the nanomaterials and thereby making it a defect free material [21]. High hardness is one of the novel properties that have been observed for many nano materials. This was mainly due to the super hard nano composites made up of nitrides, borides and carbides that are obtained by the plasma induced chemical and physical vapour deposition synthesis methods [21].

The mechanical properties of nanomaterials could lead to many potential applications in all the nano, micro and macro scales. These applications include mechanical nano-

resonators, sensors, microscope probe tips & nano tweezers for nanoscale object manipulation, wear resistance coatings, tougher and harder cutting tools, etc.

1.2.2 Magnetic Properties:

The magnetic properties of nano materials are due to the different magnetic coupling with neighbouring atoms. When the material is reduced to nano scale, ferromagnetic particles become unstable and become super paramagnetic as the surface energy supplies enough energy for the domains to switch the polarization direction spontaneously. But these paramagnets will behave indifferently than conventional paramagnets.

Magnetic nanoparticles are used in a range of applications including ferrofluids, colour imaging, bioprocessing, refrigeration as well as high storage density magnetic memory media. Giant magneto resistance (GMR) is a phenomenon observed in nanoscale multilayers consisting of a strong ferromagnet (e.g., Fe, Co) and a weaker magnetic or non- magnetic buffer (e.g., Cr, Cu); it is usually employed in data storage and sensing.

1.2.3 Optical Properties:

The optical properties of nanostructured semiconductors are highly size dependent and thus can be tuned by varying the size alone, keeping the chemical composition intact. The size dependent emission spectra of quantum dot laser are less temperature dependent make it more suitable than conventional lasers in applications. The carrier confinement and nature of electronic density of states of the quantum wells, quantum wires and quantum dots nanostructures make it preferable than bulk lasers. Rather than semiconductor lasers, metal nano particles also show the same effect.

The optical properties such as absorption and emission occur when the electron transition occurs between highest occupied orbital and lowest occupied orbital, can also show a change than that of the bulk. Another important property of nano particle is the resonance of outer electrons excited by light wavelength can give coloured nano particle solutions. These are mainly due to the surface plasmon resonance effect. The properties like photoluminescence, electroluminescence, photoemission, photo catalysis, photoconductivity etc., are different in the low dimensional nano particles [40].

1.2.4 Thermal Properties:

Many properties of the nanoscale materials have been studied deeply, including the optical, electrical, magnetic and mechanical properties. However, the studies on thermal

properties of nanomaterials are less, which is partially due to the difficulties of experimentally measuring and controlling the thermal transport in nanoscale dimensions [21].

The structure of nanomaterial, including their interfaces, the use of nano fluids is up most important in studying the thermal conductivity of nano materials. Nano fluids are generally referred to the solid-liquid composite materials, which consist of nanomaterials of size in the range 1-100 nm suspended in a liquid. The use of nano fluid instead of base fluids, to enhance the thermal transport is another application of the thermal properties of nanomaterials. The nano fluids are used in solar systems [42], engine cooling systems, heat exchangers, etc. [41]

The grain size, grain boundary, surface interactions, doping, defects etc. can affect the thermal properties. The grain size effect is greater than grain boundary. The thermal conductivity of grain boundaries can have reduced at low temperature. But the metal decorated interfaces can create additional heat channel for effective conduction. The doping can also cause a change in the thermal conductivity of nano materials [41].

1.2.5 Electrical Properties:

In bulk materials, electron can move freely in all dimensions. It is delocalized. But when the material is reduced to nano range, the localization occurs and electrons get scattered by components present in it. The reduction in particle size are accompanied by two effects: the quantum effect and the classical effect. The quantum effect is one in which the energy bands are replaced by the discrete energy states; which causes the conductivity in nano materials. When the mean free path for scattering electrons becomes comparable with size of the system, it will reduce the scattering events. This is the classical effect [21].

The electrical properties are different for different dimensional materials. For three dimensional and two dimensional nano material the ohmic contacts are possible. Whereas, One dimensional and zero dimensional nano materials have high contact resistance, which lead to the tunnelling of electrons. Thus, it makes the conductivity in nano regime. These are usually used in the electrical coupling of gold nano particles; where it is connected each other by organic molecule. [21]

1.2.6 Acoustic Properties:

Many of the material properties like mechanical, optical, chemical etc. are observed in nano scales. Materials interact strongly with radiation that has a wavelength comparable with their internal structure and /or dimensions [21]. When the material is reduced to nano size, their

interaction with radiation within the visible region, ultra violet and x-ray regions are possible. The low dimensional nano materials can have superior piezoelectric properties and excellent mechanical properties can exhibit acoustic properties to some extent. To study the acoustic property, the study of the interaction of these nano particles with a high wavelength that ranges from microns to kilometre have to be done. Despite the rapid progress in the related field, discussion of acoustic properties is limited for the case of nanomaterial [43].

But the properties of nanomaterials in many cases are different from higher dimensional materials, acoustic waves can have a distinct indirect effect such as the case of seismic waves [21].

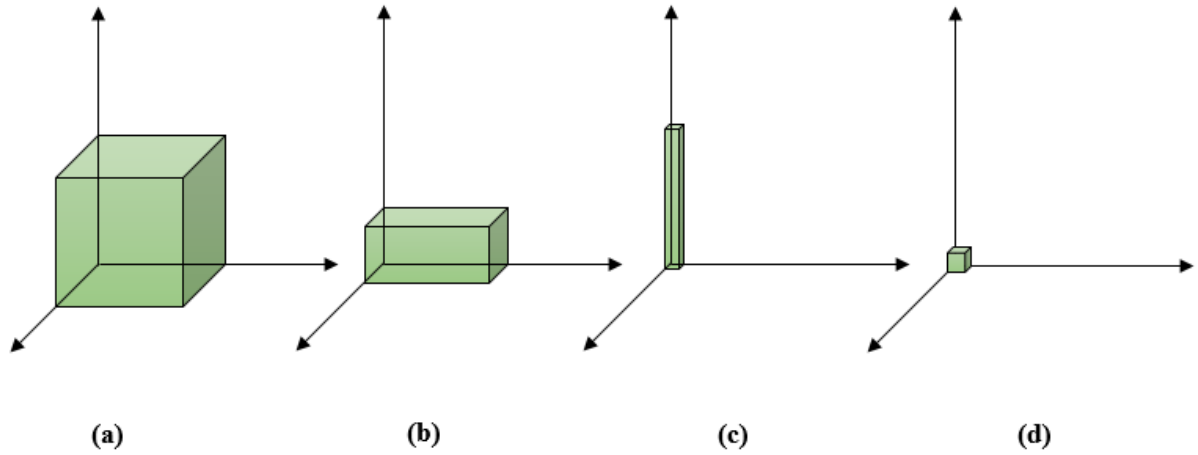

Figure 1.2: Different dimensional nano structures (a) 3D nano materials (b) 2D nano materials (c) 1D nano materials (d) 0D nano materials [22]

1.3 Synthesis of nano materials

Generally, there are two types of synthesis methods are available. They are 'Bottom-up' method and 'Top-down' approach.

1.3.1 Top-down method of synthesis

In this method, the bulk system is crushed to the nano scale by mechanical or chemical means. In this process, additional molecules can also be added to synthesis a compound nano material. Thermolysis, RF plasma, atomic force manipulation, lithography (electron beam lithography/ photo lithography/ two photon lithography), high energy wet ball milling, aerosol, etc. are various methods that fall under top-down approach. These type of synthesis methods are cheap and quick. It enables miniaturization of the bulk materials with desired structure and required properties. However, the processing time is very large and is not suitable for large

scale production. The end products may also bear some structural defects on its surface. The nanomaterials synthesised through such methods are extremely appropriate for high quality optical mirrors. [23]

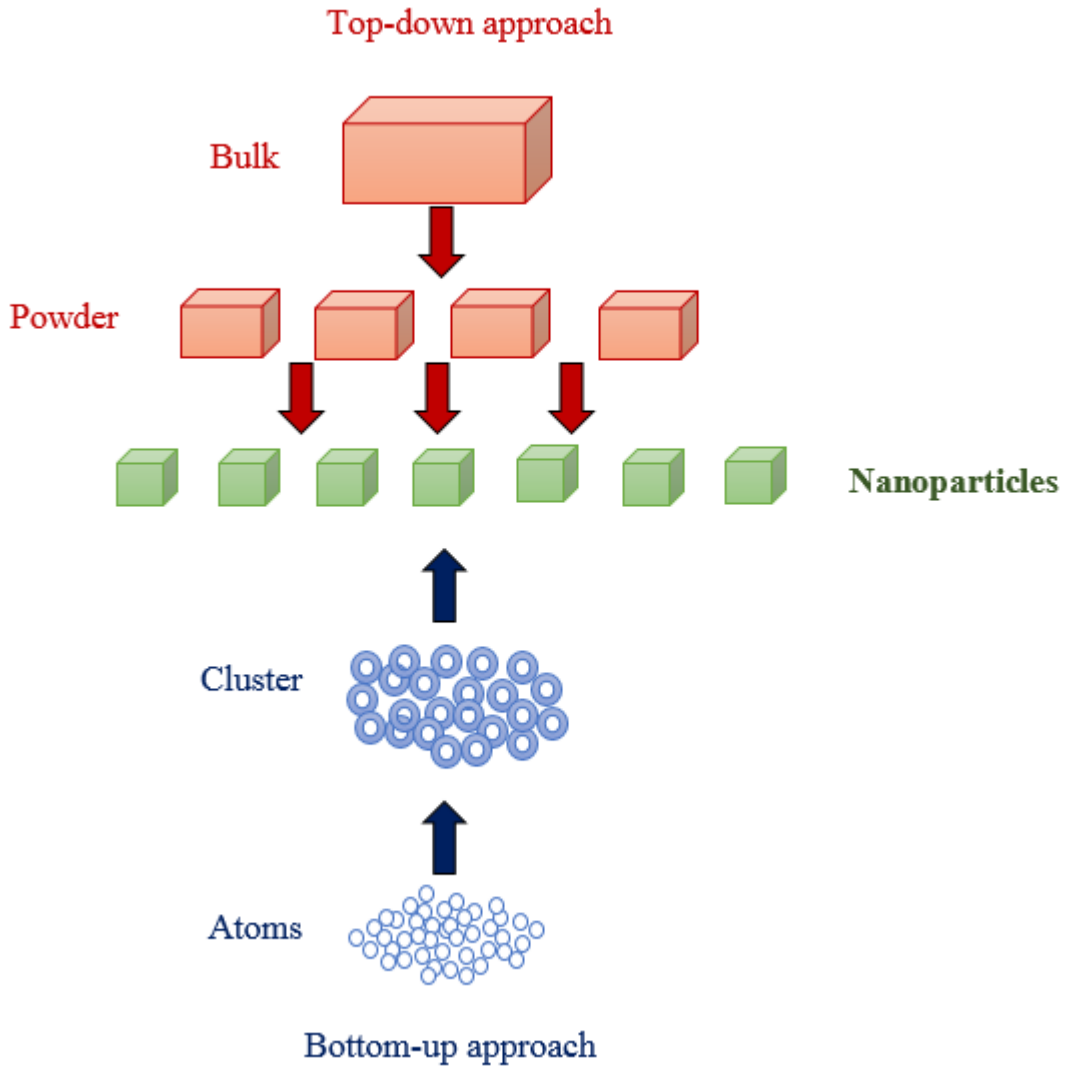

Figure 1.3: Schematic representation of 'top-down' and 'bottom-up' approaches of nanomaterial synthesis [24]

1.3.2 Bottom-up method of synthesis

In bottom –up approach, the nano scaled materials are built up from the bottom, that is atom-by-atom, molecule-by-molecule or cluster-by-cluster. Here the materials are developed via self-assembly, which is triggered by some chemical or physical means. Though this synthesis method is more expensive, it is much faster than the top-down method. Hence it is used for commercial production of nano powders. Chemical method, pulse laser deposition technique, hydrothermal synthesis, sol-gel method, template assisted sol gel method, self-

assembly technique, co-precipitation, etc. are some examples of bottom- up synthesis method. The as synthesised nano materials are well fit for creating display panels, experimental atomic or molecular devices, etc. [23]

1.4 Application of nano materials

Due to their large signal to noise ratio and other feasible properties of nano sized materials, their interaction with other particles can pave a new route for the development of some important technologies both in the field of medical and non-medical. For a past few decades, several extensive studies have been carried out in the area of nano science and nano technology. This is because of their scope related to human health and existence of ones in the earth. They can have their diverse applications in the field of:

- Sensors
- Anticancer properties
- Electronics
- Biomedicine antibacterial coatings
- Photocatalytic activity
- Water decontamination
- Solar desalination
- Drug delivery
- Dye sensitization

1.5 Silver nanoparticles

Among nano materials metal nano particles have promising applications. Silver is a noble metal with highest thermal and electrical conductivity, which make them appropriate for many fascinating applications. It can be used as interconnects in electronic devices including computers, mobile phones, automobile appliances, cosmetics, medical devices, imaging techniques, water and environment disinfectants [44] Several researches have already done to determine the material properties of silver nanoparticles. One of the most important property of preferring silver nano particles are due to their plasmonic property and reactivity towards SERS (Surface enhanced Raman scattering). Due to the excitation of localized surface plasmon resonance (LSPR), silver nano particles have high scattering efficiency, thereby they can

introduce diverse plasmonic applications [25]. These LSPR in turn depends upon the size of the particle, the shape and the environment at the resonance wavelength [26][27].

1.6 Silver nanoparticles integrated Graphene nano sheet

The increase in carcinogenic diseases are mostly due to the over dosage of pesticides and other chemicals. As a part of commercialization, millions of chemicals are produced every year. Most of these chemicals are banned by the countries due to their over dosage and to protect the life on the earth. Among these pesticides, thiram is widely utilized in agricultural production have caused serious pesticide pollution [29].

Here, the silver nanoparticles have been homogeneously integrated on the surface of the Graphene Oxide. It is based on the ability of graphene to vary the plasmonic properties of metal nanostructures. The prepared reduced Graphene oxide/silver nanocomposites act as a SERS substrate by a simple and efficient method, in which $AgNO_3$ is reduced anhydrous ethylene glycol (EG) with (polyvinylpyrrolidone) as a dispersing agent. The mechanism and role of the (polyvinylpyrrolidone) (PVP) in the growth of rGO/Ag nanocrystals are given and discussed.

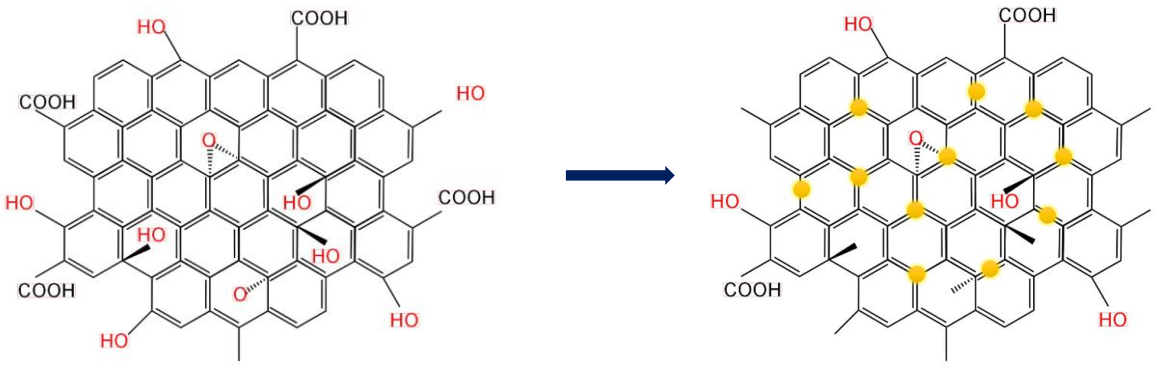

(a) **(b)**

Figure 1.6: (a) GO nanosheet (b) Ag+ ions integrated on GO sheet

The integration of metal nano particles on the suitable support stand can improve its efficiency by removing the agglomeration and coalescence of NPs. The metals usually exhibit charge transfer ability, superior mechanical strength, exceptionally high surface area and thermal stability. When these metal nano particles are assembled on the sp^2 hybridized graphene sheet, it can exhibit fascinating optical and electrical properties, extraordinary thermal stability due to the improved interaction between metal nanoparticles with the carbon

network. Since the graphene structure has already reported its efficiency in providing adsorption ability and more active sites, their interaction with metal nano particles can be seen enhanced than in bare nanoparticles [30-32].

The characterisation of as prepared GO/Ag nanocomposite can be done using X- ray diffraction, UV-Visible analysis, SEM-EDX, FE-SEM, HRTEM and Raman analysis.

1.7 Scope of the work

Among various techniques, the Surface enhances Raman spectroscopy (SERS) plays a vital role in the plasmonic applications. In this project, the study of sensing nature of nano sized composites was carried out using highly sensitive technical analysis based on Surface Enhanced Raman scattering (SERS). Since SERS can trace of particles with enhanced mechanism. The graphene- metal nano composites can exhibit potential SERS capabilities due to the electromagnetic field enhancement from the metal nanostructures and the chemical enhancement arising as a result of the strong π-π interactions in graphene [34]. When we use silver integrated GO SERS substrate, it can enhance their activity towards the targeted molecule. The trapping capability of silver substrate on certain functional groups can also be incorporated to explore for the fruitful applications. Moreover, the SERS is a rapid and non-destructive technique can give the 'finger print like' information about an analyte, it is considered as the best option for on-site monitoring of pesticides and such chemicals in real applications [9][37-39].

In this work, the SERS performance of the rGO/Ag nano particle against the chemical dye 'crystal violet' and the pesticide 'Thiram' as the probe molecules are examined, which indicates that the rGO/Ag as a SERS substrate have excellent sensitivity and reproducibility. The antibacterial activity of rGO/Ag nanocomposite against two bacterial strains: E. coli and staphylococcus are also studied.

REFERENCE

1. Nayak, Pragati, and Hitesh Solanki. "Pesticides and Indian agriculture—a review." *Int J Res Granthaalayah* 9 (2021): 250-63.

2. Li, Yongyu, Yunyun Sun, Yankun Peng, Sagar Dhakal, Kuanglin Chao, and Qiaoqiao Liu. "Rapid detection of pesticide residue in apple based on Raman spectroscopy." In *Sensing for agriculture and food quality and safety IV*, vol. 8369, pp. 128-133. SPIE, 2012.

3. Raghu, P., T. Madhusudana Reddy, BE Kumara Swamy, B. N. Chandrashekar, K. Reddaiah, and M. Sreedhar. "Development of AChE biosensor for the determination of methyl parathion and monocrotophos in water and fruit samples: A cyclic voltammetric study." *Journal of Electroanalytical Chemistry* 665 (2012): 76-82.

4. Chai, Lian-Kuet, and Fatimah Elie. "A rapid multi-residue method for pesticide residues determination in white and black pepper (Piper nigrum L.)." *Food Control* 32, no. 1 (2013): 322-326.

5. Lavagnini, Irma, Alessandro Urbani, and Franco Magno. "Overall calibration procedure via a statistically based matrix-comprehensive approach in the stir bar sorptive extraction–thermal desorption–gas chromatography–mass spectrometry analysis of pesticide residues in fruit-based soft drinks." *Talanta* 83, no. 5 (2011): 1754-1762.

6. Tsochatzis, Emmanouil D., Urania Menkissoglu-Spiroudi, Dimitrios G. Karpouzas, and Roxani Tzimou-Tsitouridou. "A multi-residue method for pesticide residue analysis in rice grains using matrix solid-phase dispersion extraction and high-performance liquid chromatography–diode array detection." *Analytical and Bioanalytical Chemistry* 397, no. 6 (2010): 2181-2190.

7. Fernández, M., Y. Picó, and J. Manes. "Determination of carbamate residues in fruits and vegetables by matrix solid-phase dispersion and liquid chromatography–mass spectrometry." *Journal of Chromatography A* 871, no. 1-2 (2000): 43-56.

8. Shende, Chetan, Alan Gift, Frank Inscore, Paul Maksymiuk, and Stuart Farquharson. "Inspection of pesticide residues on food by surface-enhanced Raman spectroscopy." In *Monitoring food safety, agriculture, and plant health*, vol. 5271, pp. 28-34. SPIE, 2004.

9. He, Lili, Tuo Chen, and Theodore P. Labuza. "Recovery and quantitative detection of thiabendazole on apples using a surface swab capture method followed by surface-enhanced Raman spectroscopy." *Food chemistry* 148 (2014): 42-46.

10. Pang, Shintaro, Theodore P. Labuza, and Lili He. "Development of a single aptamer-based surface enhanced Raman scattering method for rapid detection of multiple pesticides." *Analyst* 139, no. 8 (2014): 1895-1901.
11. Kneipp, Janina, Harald Kneipp, and Katrin Kneipp. "SERS—a single-molecule and nanoscale tool for bioanalytics." *Chemical Society Reviews* 37, no. 5 (2008): 1052-1060.
12. Hering, Katharina, Dana Cialla, Katrin Ackermann, Thomas Dörfer, Robert Möller, Henrik Schneidewind, Roland Mattheis, Wolfgang Fritzsche, Petra Rösch, and Jürgen Popp. "SERS: a versatile tool in chemical and biochemical diagnostics." *Analytical and bioanalytical chemistry* 390, no. 1 (2008): 113-124.
13. Baibarac, M., I. Baltog, L. Mihut, A. Matea, and S. Lefrant. "Nonlinear features of surface-enhanced Raman scattering revealed under non-resonant and resonant optical excitation." *Journal of Optics* 16, no. 3 (2014): 035003.
14. Guerrini, Luca, Santiago Sanchez-Cortes, Victor L. Cruz, Sonia Martinez, Sandra Ristori, and Alessandro Feis. "Surface-enhanced Raman spectra of dimethoate and omethoate." *Journal of Raman Spectroscopy* 42, no. 5 (2011): 980-985.
15. Wan, Fu, Haiyang Shi, Weigen Chen, Zhaoliang Gu, Lingling Du, Pinyi Wang, Jianxin Wang, and Yingzhou Huang. "Charge transfer effect on raman and surface enhanced raman spectroscopy of furfural molecules." *Nanomaterials* 7, no. 8 (2017): 210.
16. Xu, Weigao, Nannan Mao, and Jin Zhang. "Graphene: a platform for surface-enhanced Raman spectroscopy." *Small* 9, no. 8 (2013): 1206-1224.
17. Guozhong Cao, Ying Wang , "Nanostructures and Nanomaterials Synthesis, Properties, and Applications", 2011
18. Fiiipponi, Luisa, and Duncan Sutherland, eds. Nanotechnologies: principles, applications, implications and hands-on activities: A compendium for educators. European Union, Directorate General for Research and Innovation, 2012.
19. Bharat Bhushan, Springer Handbook of Nanotechnology: 3rd revised and extended edition, Springer, 2010.
20. G Ramalingam, P Kathiragamanthan, G Ravi, T Elangovan, B A kumar, N Manivannan, K Kasinathan," Quantum confinement effect of 2D nanomaterials", 2019
21. Santhi A, The Nanoscope: An introduction to Nanoscience and Nanophotonics, Medtech, 2016
22. Kebede, Mekuriaw Assefa, and Toyoko Imae. "Low-dimensional nanomaterials." In Advanced Supramolecular Nanoarchitectonics, pp. 3-16. William Andrew Publishing, 2019.

23. B P Singh, “Nanoscience and nanotechnologies: opportunities and uncertainities”, The royal society & the royal Academy of Engineering, 30 July 2004

24. Anker, Jeffrey N., W. Paige Hall, Olga Lyandres, Nilam C. Shah, Jing Zhao, and Richard P. Van Duyne. "Biosensing with plasmonic nanosensors." Nanoscience and Technology: A Collection of Reviews from Nature Journals (2010): 308-319.

25. Zhao, Yuan, and Yanwu Zhu. "Graphene-based hybrid films for plasmonic sensing." *Nanoscale* 7, no. 35 (2015): 14561-14576.

26. Sönnichsen, Carsten, Björn M. Reinhard, Jan Liphardt, and A. Paul Alivisatos. "A molecular ruler based on plasmon coupling of single gold and silver nanoparticles." Nature biotechnology 23, no. 6 (2005): 741-745.

27. Yang, Zhiqiang, Haijun Qian, Hongyu Chen, and Jeffrey N. Anker. "One-pot hydrothermal synthesis of silver nanowires via citrate reduction." Journal of colloid and interface science 352, no. 2 (2010): 285-291.

28. J Anker, W Hall, O Lyandres, N Shah, J Zhao, R Van Duyne, Nature Mater., 2008, 7, 442

29. Zhang L, Wang B, Zhou X, “Synthesis of silver nanocubes as a SERS substrate for the determination of pesticide paraoxon and thiram”, Spectrochimica Acta Part A: Molecular and Biomolecular Spectroscopy 121, (2014), 63-69

30. Yin, Huajie, Hongjie Tang, Dan Wang, Yan Gao, and Zhiyong Tang. "Facile synthesis of surfactant-free Au cluster/graphene hybrids for high-performance oxygen reduction reaction." *Acs Nano* 6, no. 9 (2012): 8288-8297.

31. Yu, Xiaoqing, Wensi Zhang, Panpan Zhang, and Zhiqiang Su. "Fabrication technologies and sensing applications of graphene-based composite films: advances and challenges." *Biosensors and Bioelectronics* 89 (2017): 72-84.

32. Li, Y.; Zhang, P.; Ouyang, Z.; Zhang, M.; Lin, Z.; Li, J.; Su, Z.; Wei, G. Nanoscale Graphene Doped with Highly Dispersed Silver Nanoparticles: Quick Synthesis, Facile Fabrication of 3D Membrane-Modified Electrode, and Super Performance for Electrochemical Sensing. Adv. Funct. Mater. 2016, 26 (13), 2122–2134

33. Engel, Michael, Mathias Steiner, Antonio Lombardo, Andrea C. Ferrari, Hilbert V. Löhneysen, Phaedon Avouris, and Ralph Krupke. "Light–matter interaction in a microcavity-controlled graphene transistor." *Nature communications* 3, no. 1 (2012): 1-6.

34. Lee, Jisook, Konstantin S. Novoselov, and Hyeon Suk Shin. "Interaction between metal and graphene: dependence on the layer number of graphene." *ACS nano* 5, no. 1 (2011): 608-612.

35. Yi, Congwen, Tong-Ho Kim, Wenyuan Jiao, Yang Yang, Anne Lazarides, Kurt Hingerl, Giovanni Bruno, April Brown, and Maria Losurdo. "Evidence of plasmonic coupling in gallium nanoparticles/graphene/SiC." *Small* 8, no. 17 (2012): 2721-2730.
36. Gao, Nan, Ting Yang, Tao Liu, Yu Zou, and Jiang Jiang. "Graphene oxide wrapped individual silver nanocomposites with improved stability for surface-enhanced Raman scattering." *RSC Advances* 5, no. 69 (2015): 55801-55807.
37. Liu, Bin, Peng Zhou, Xiaoming Liu, Xin Sun, Hao Li, and Mengshi Lin. "Detection of pesticides in fruits by surface-enhanced Raman spectroscopy coupled with gold nanostructures." *Food and Bioprocess Technology* 6, no. 3 (2013): 710-718.
38. Liu, Bianhua, Guangmei Han, Zhongping Zhang, Renyong Liu, Changlong Jiang, Suhua Wang, and Ming-Yong Han. "Shell thickness-dependent Raman enhancement for rapid identification and detection of pesticide residues at fruit peels." *Analytical chemistry* 84, no. 1 (2012): 255-261.
39. Li, Xiaozhou, Su Zhang, Zhuang Yu, and Tianyue Yang. "Surface-enhanced Raman spectroscopic analysis of phorate and fenthion pesticide in apple skin using silver nanoparticles." *Applied spectroscopy* 68, no. 4 (2014): 483-487.
40. Bhagyaraj, Sneha Mohan, and Oluwatobi Samuel Oluwafemi. "Nanotechnology: the science of the invisible." In *Synthesis of inorganic nanomaterials*, pp. 1-18. Woodhead Publishing, 2018.
41. Qiu, Lin, Ning Zhu, Yanhui Feng, Efstathios E. Michaelides, Gaweł Żyła, Dengwei Jing, Xinxin Zhang, Pamela M. Norris, Christos N. Markides, and Omid Mahian. "A review of recent advances in thermophysical properties at the nanoscale: From solid state to colloids." *Physics Reports* 843 (2020): 1-81.
42. Mahian, Omid, Ali Kianifar, Saeed Zeinali Heris, Dongsheng Wen, Ahmet Z. Sahin, and Somchai Wongwises. "Nanofluids effects on the evaporation rate in a solar still equipped with a heat exchanger." *Nano energy* 36 (2017): 134-155.
43. Peng, Chang, Mengyue Chen, James B. Spicer, and Xiaoning Jiang. "Acoustics at the nanoscale (nanoacoustics): A comprehensive literature review. Part I: Materials, devices and selected applications." *Sensors and Actuators A: Physical* 332 (2021): 112719.
44. Maaz, Khan (2018). *Silver Nanoparticles - Fabrication, Characterization and Applications || Synthesis of Silver Nanoparticles., 10.5772/intechopen.71247(Chapter 1),* – .doi:10.5772/intechopen.75363

CHAPTER 2

GENERAL SYNTHESIS METHODS

2.1 Synthesis of Graphene Oxide (GO)

The synthesis of graphene oxide and its derivatives with desired morphology and reactivity is mainly dependent upon properties like size, shape, functional groups attached to the surface, etc. The structure of one dimensional graphene consists of a single-atom layer with sp^2 hybridized carbon strands. They usually possess fewer defects. While GO has a two dimensional structure with hydrogen, oxygen and carbon molecule in sp^2 hybridization as well as sp^3 hybridization. The synthesis of reduced GO structures can be divided into two: top-down method of synthesis or bottom-up approach of synthesis. The bottom-up approach is difficult for commercial applications as it consumes more time and is likely to have structural defects. In the case of the top-down approach, the synthesis of reduced form of GO with both sp^2 and sp^3 hybridized states is easier. Different synthesis methods are:

2.1.1 Synthetic Methods for Graphene Oxide

a) Brodie's method

In Brodie's method, the thermal treatment of graphene gives GO with conjugated epoxy and hydroxyl groups. Since it is a temperature assisted method, the incorporation of oxygen functional groups can prevent its complete restoration. The synthesis method is as follows:

Fuming nitric acid (200 mL) is added into a flask with a cooling jacket and cooled to 0°C in a cryostat bath. The graphite powder (10 g) is introduced into the flask and thoroughly dispersed to avoid agglomeration. Next, potassium chlorate (80 g) is slowly added for 1 h, and the reaction mixture is stirred for 21 h at 0°C. Special caution is necessary during addition of potassium chlorate since explosions may occur [3]. Once the reaction is complete, the mixture is diluted in distilled water and vacuum filtered until the pH of the filtrate is neutral [1].

b) Staudenmaier's method

It was in 1898 that Staudenmaier improved the Brodie's reaction by adding H_2SO_4, to increase the acidity of the mixture, and several aliquots of solid $KClO_3$, over the course of the reaction. Brodie and Staudenmaier method generates ClO_2 toxic gas which rapidly decomposes

in air causing explosions. These modifications led to a more oxidized graphitic material and a simplification of the reaction [2].

c) Hummers method

In 1958, Hummers and Offeman proposed a simple, effective and faster way to oxide graphite, improving the safety of operational conditions with a drastic reduction in time, from 10 to 2 days. They mixed graphite flakes with concentrated sulfuric acid (H_2SO_4), sodium nitrate ($NaNO_3$) and potassium permanganate ($KMnO_4$) to obtain a brownish grey pasty. The suspension was diluted with water. Hydrogen peroxide (H_2O_2) was added to get a higher oxidation degree and to eliminate manganese from the dispersion (yellow-brown mixture). Finally, the sample was filtered and washed with warm water. They achieved the same degree of oxidation reported by Staudenmaier, however, the amount of GO synthesised was very little. The drawback of this method is that it is rather time-consuming when it comes to the separation and purification process [3].

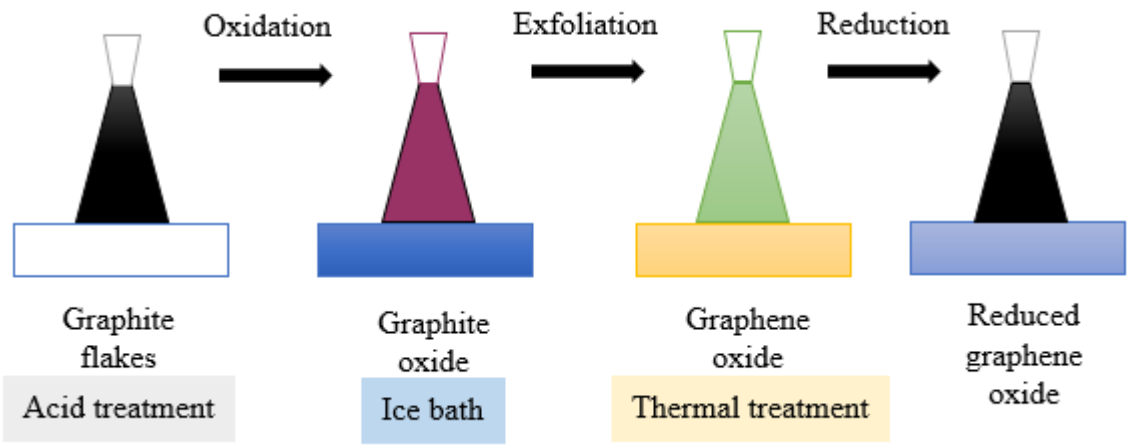

Figure 2.1: synthesis of rGO from graphite flakes

d) Tour Method

It was in 2010, Tour's group at Rice University proposed this method as an improvement of Hummer's method. They substituted the sodium nitride with phosphoric acid in a mixture of H_2SO_4/H_3PO_4 (9:1) and increased the amount of $KMnO_4$. Toxic gases such as NO_2, N_2O_4 or ClO_2 are not produced here. The authors claim that the presence of phosphoric acid generates a more intact graphitic basal plane. The advantage of the Tour method is that

produces graphene oxide having a higher hydrophilic degree, in contrast to the GO produced by Hummers method. Thus, the resultant graphene oxide is more oxidized and soluble [4].

2.1.2 Free-Water Oxidation Method

Free-Water Oxidation method relies on the reaction between expanded graphite and an oxidizing agent in a free-water medium. They are of 3 types. Since the inorganic carbon is inert at room temperature, its solubilization/dispersion in a solvent requires the presence of a strong protic acid or mixture of warm acids, such as sulphuric or nitric acid. Moreover, in this method, a strong oxidizing agent, such as potassium permanganate ($KMnO_4$), ensures the bonding of oxygen functionalities to inorganic carbons [5].

a) Sun Method

In 2013, Sun and Fugetsu at Hokkaido University introduced a more direct method to produce graphene oxide. They used expanded graphite as carbon precursor. The potassium permanganate had twofold effects, acting as an intercalating agent as well as an oxidizing agent. The intercalation of KMnO4 between graphitic layers produced a further spontaneous expansion which looks like a foam of graphitic material. The reaction in carried out in an acidic medium with sulfuric acid. The ratio of Graphite:H_2SO_4 was reduced to 1:20 and additional reagents were eliminated from the reaction procedure. For this reason, Sun protocol can be considered as one of the first green procedure, among the wet synthesis methods [6].

b) Peng Method

It was in 2015, that Peng and co-workers proposed a scalable and green method to produce graphene oxide, using potassium ferrate (K_2FeO_4) as a strong oxidant. This compound avoids the introduction of heavy metals or the formation of toxic gases during the preparation. In this method, a mixture of graphitic flakes and K_2FeO_4 dispersed in concentrated sulphuric acid, are loaded into a reactor and stirred for 1h at room temperature. The product is washed through repeated centrifugation to obtain highly water soluble graphene oxide [7].

c) 4-Steps Method

This method is derived from the basic exfoliation-oxidation procedure and was improved by Pendolino and co-workers [8]. In this method the overall reaction consists of 4 steps controlled by temperature. The reaction involves two paths. In the first step the $KMnO_4$

dispersed in concentrated H_2SO_4 get oxidized, resulting in a pasty slurry. The second step (warm) consists of the exfoliation of graphite. Since the production of graphene oxide is limited by temperature, the entire process is done in a water bath around 30^oC. The exfoliation is suppressed at a lower temperature resulting in the formation of graphite oxide (cold). The third step is hydrolysis which is carried out at 90^oC for 1 h. Finally, the purification is performed by centrifugation using warm water. Through the 4-Steps method two different products can be synthetized by just controlling the temperature throughout the reaction.

2.2 Synthesis of reduced Graphene Oxide/Silver (rGO/Ag) nano composites

An efficient synthesis method is of high interest in case of silver nano materials due to their extensive applications. The main challenge that one has to face during the synthesis of silver nano particles is in controlling their physical properties such as size, shape, morphology, chemical composition or type, crystal structure etc. There are numerous methods aimed at doing the same.

2.2.1 Chemical method

a) Polyol method

Reducing silver nitrate with ethylene glycol using the capping agent polyvinylpyrrolidone (PVP) for the synthesis of monodispersed solution of silver nanocubes is an example of polyol process [9]. Here ethylene glycol plays the role of both the reducing agent as well the solvent. The role of PVP and its relative molar ratio to silver nitrate along with additive formaldehyde, NaOH is important in finalizing the geometric shape and size of the product. It is evident that the size of silver nanocubes can be tuned by controlling the experimental conditions.

b) Precursor injection technique

The injection rate and the reaction temperature play important roles for the production of uniform sized Ag-NPs [10]. Rapid nucleation can be induced effectively in a short period of time by injecting the precursor solution into a hot solution. This will ensure the reduced size and narrower size distribution of Ag-NPs. The synthesis of spherical Ag-NPs with controllable size and high monodispersity can be achieved by introducing this precursor injection technique to the polyol process. Particles of size 17±2 nm were obtained at an injection rate of 2.5 mLs -1, carried out at 100^oC. Monodispersed Ag-NPs have been prepared in a simple oleylamine-liquid paraffin system [11] by using this technique.

2.2.2 Physical method

A common technique in this method is the evaporation-condensation process carried out in a tube furnace at atmospheric pressure. The drawbacks of this technique include large space requirement for the tube furnace, consumption of large amount of energy, raising the environmental temperature around the source material and large amount of time for achieving thermal stability. Powdered Ag-NPs with narrow particle size distribution can be prepared using thermal decomposition method [12]. It is noteworthy that Jung et al. [13] reported that a small ceramic heater with local heating area can be used for the synthesis of metal NPs by evaporating the source materials under the flow of a carrier gas i.e., air. The geometric mean diameter, geometric standard deviation and total concentration of the spherical NPs without agglomeration increases with increase in the heater temperature. Interestingly Tien et al. [14] has advocated for the synthesis of Ag-NPs using electrical discharge machining (EDM) without the addition of any surfactants where pure silver wires are submerging in deionized water and treated as electrodes.

2.2.3 Photochemical method

The photo-assisted synthesis (photo-reduction) of silver is another method used for the preparation of Ag-NPs. It is a fast and efficient method for producing electrons. The preparation of stable nanoparticles of Ag-NPs can be done by irradiation of a reaction mixture with a light source (laser or lamp) in the presence of photoreducing agents or a photo active spieces. There is no need to add stabilizers or surfactants here [15−17]. Their size and the time needed for their preparation are directly proportional to the irradiation power of the light source. For example, with a low-power lamp (4 W), irradiation for 9 h is needed to produce 19 nm diameter Ag-NPs,[17] while with a stronger source (150 W), the reaction takes only 45 min. However, in the latter case, the Ag-NPs are polydisperse and smaller than when they are prepared using a lower-energy lamp [17]. The efficiency of light source has prime importance in this method as it is the energy that gets absorbed by the catalysts to generate free electrons.

2.2.4 Biological method

Recently biosynthesis (or Green synthesis) of the nanoparticles has received considerable attention. The green synthesis of inorganic materials are usually done using microorganisms such as bacteria [19], algae [20], yeast [21], and fungi [22] and plant extracts. Various bacterial strains such as Bacillus amyloliquefaciens, Acinetobacter calcoaceticus, Pseudomonas aeruginosa, Escherichia coli and Bacillus licheniformis have been used

effectively for the synthesis of silver nanoparticles. The ready availability of plants with large variety of active functional groups make them suitable for reduction of silver ions.

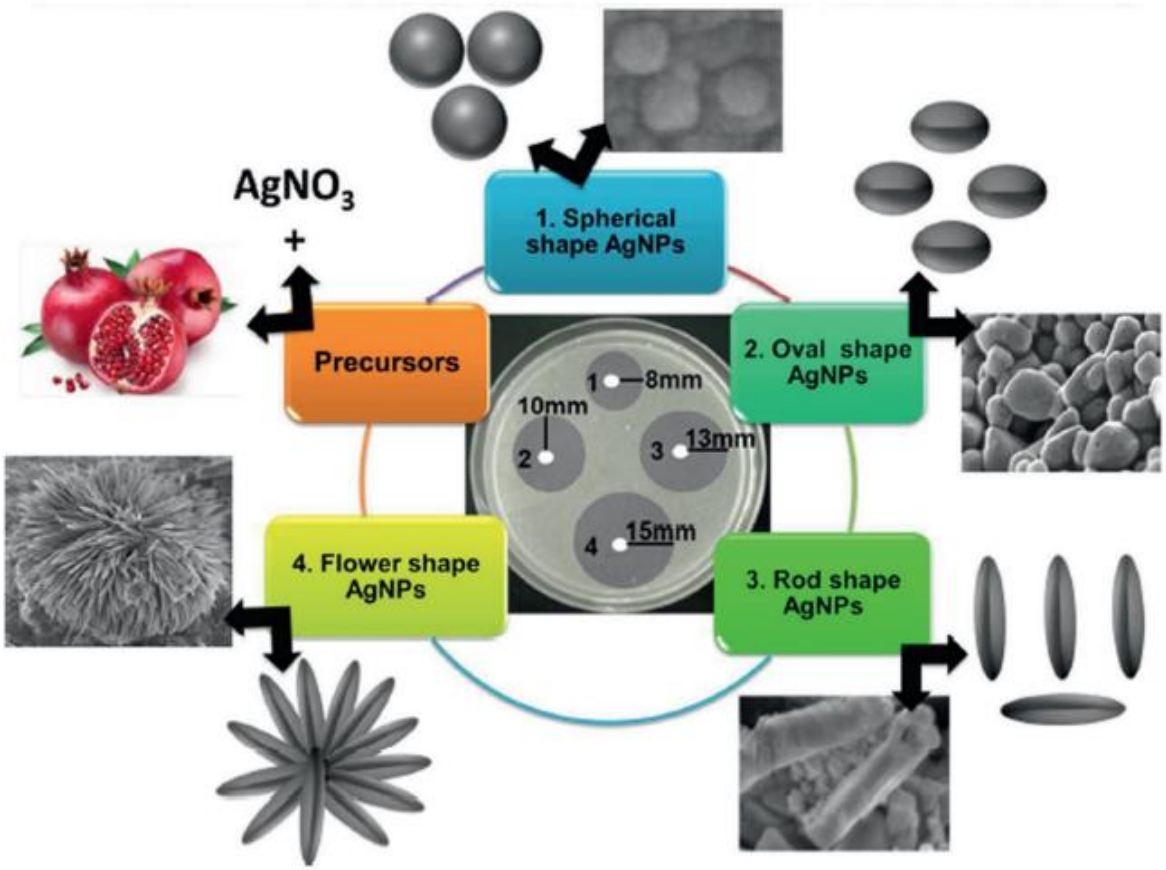

Figure 2.2: Biosynthesis of Ag nano particles with different shape and their antibacterial activity [23]

Each plant parts like leaves, stem, roots, seeds, bark etc can be used for synthesis. The procedure begins with the collection and cleaning of the plant part of interest. Then it should be dried in the shade for 10-15 days and pulverized using a blender. The powdered plant part is boiled in deionized water, to obtain the plant broth. Then is then filtered out in such a way that, no insoluble materials are seen. A few mL of this plant extract is added to silver nitrate solution with required concentration. The reduction of silver ion to silver oxide can be observed from the colour change accompanying them. The plants like *Alternanthera dentate, Cymbopogon citratus, Argyreia nervosa, phlomis, Aloe vera , Carica papaya, Nelumbo nucifera, Moringa oleifera, Ziziphora tenuior, Centella asiatica, Vitex negundo, Swietenia mahagoni, Boerhavia diffusa, Cocos nucifera, Brassica rapa, Melia dubia, Pogostemon benghalensis, Garcinia mangostana, Psoralea corylifolia etc. are commonly used for green synthesis* [18].

REFERENCE

1. Brodie, B. C. "Hydration behavior and dynamics of water molecules in graphite oxide." *Ann Chim Phys* 59 (1860): 466-72.

2. Staudenmaier L (1898) Verfahren zur Darstellung der Graphitsäure. Ber Dtsch Chem Ges 31(2):1481–1487

3. William, S., J. R. Hummers, and Richard E. Offeman. "Preparation of graphitic oxide." *J. Am. Chem. Soc* 80, no. 6 (1958): 1339-1339.

4. Marcano, Daniela C., Dmitry V. Kosynkin, Jacob M. Berlin, Alexander Sinitskii, Zhengzong Sun, Alexander Slesarev, Lawrence B. Alemany, Wei Lu, and James M. Tour. "Improved synthesis of graphene oxide." *ACS nano* 4, no. 8 (2010): 4806-4814.

5. Pendolino, Flavio, and Nerina Armata. "Synthesis, characterization and models of graphene oxide." In *Graphene oxide in environmental remediation process*, pp. 5-21. Springer, Cham, 2017.

6. Sun, Ling, and Bunshi Fugetsu. "Mass production of graphene oxide from expanded graphite." *Materials Letters* 109 (2013): 207-210.

7. Peng, Li, Zhen Xu, Zheng Liu, Yangyang Wei, Haiyan Sun, Zheng Li, Xiaoli Zhao, and Chao Gao. "An iron-based green approach to 1-h production of single-layer graphene oxide." *Nature communications* 6, no. 1 (2015): 1-9.

8. Pendolino, Flavio, Nerina Armata, Tiziana Masullo, and Angela Cuttitta. "Temperature influence on the synthesis of pristine graphene oxide and graphite oxide." *Materials Chemistry and Physics* 164 (2015): 71-77.

9. Link, S., Zz L. Wang, and M. A. El-Sayed. "Alloy formation of gold− silver nanoparticles and the dependence of the plasmon absorption on their composition." *The Journal of Physical Chemistry B* 103, no. 18 (1999): 3529-3533.

10. Fievet, F., J. P. Lagier, and M. Figlarz. "Preparing monodisperse metal powders in micrometer and submicrometer sizes by the polyol process." *Mrs Bulletin* 14, no. 12 (1989): 29-34.

11. Yamamoto, Tetsushi, Yuji Wada, Takao Sakata, Hirotaro Mori, Masaki Goto, Shingo Hibino, and Shozo Yanagida. "Microwave-assisted preparation of silver nanoparticles." *Chemistry letters* 33, no. 2 (2004): 158-159.

12. Lee, Don Keun, and Young Soo Kang. "Synthesis of silver nanocrystallites by a new thermal decomposition method and their characterization." *Etri Journal* 26, no. 3 (2004): 252-256.

13. Jung, Jae Hee, Hyun Cheol Oh, Hyung Soo Noh, Jun Ho Ji, and Sang Soo Kim. "Metal nanoparticle generation using a small ceramic heater with a local heating area." *Journal of aerosol science* 37, no. 12 (2006): 1662-1670.

14. Tien, Der-Chi, Kuo-Hsiung Tseng, Chih-Yu Liao, Jen-Chuen Huang, and Tsing-Tshih Tsung. "Discovery of ionic silver in silver nanoparticle suspension fabricated by arc discharge method." *Journal of alloys and compounds* 463, no. 1-2 (2008): 408-411.

15. Jia, Huiying, Jiangbo Zeng, Wei Song, Jing An, and Bing Zhao. "Preparation of silver nanoparticles by photo-reduction for surface-enhanced Raman scattering." *Thin Solid Films* 496, no. 2 (2006): 281-287.

16. Tsuji, Takeshi, Yuuki Okazaki, and Masaharu Tsuji. "Photo-induced morphological conversions of silver nanoparticles prepared using laser ablation in water—Enhanced morphological conversions using halogen etching." *Journal of Photochemistry and Photobiology A: Chemistry* 194, no. 2-3 (2008): 247-253.

17. Kshirsagar, Prakash, Shiv Shankar Sangaru, Maria Ada Malvindi, Luigi Martiradonna, Roberto Cingolani, and Pier Paolo Pompa. "Synthesis of highly stable silver nanoparticles by photoreduction and their size fractionation by phase transfer method." *Colloids and Surfaces A: Physicochemical and Engineering Aspects* 392, no. 1 (2011): 264-270.

18. Maaz, Khan (2018). *Silver Nanoparticles - Fabrication, Characterization and Applications || Synthesis of Silver Nanoparticles., 10.5772/intechopen.71247(Chapter 1),* – .doi:10.5772/intechopen.75363

19. Samadi, Nasrin, Donya Golkaran, Ali Eslamifar, Hosein Jamalifar, Mohammad Reza Fazeli, and Farzaneh Aziz Mohseni. "Intra/extracellular biosynthesis of silver nanoparticles by an autochthonous strain of proteus mirabilis isolated fromphotographic waste." *Journal of Biomedical Nanotechnology* 5, no. 3 (2009): 247-253.

20. El-Rafie HM, El-Rafie MH, Zahran MK. Green synthesis of silver nanoparticles using polysaccharides extracted from marine macro algae. *Carbohydrate Polymers*. 2013;96:403-410

21. Jha, Anal K., and K. Prasad. "Yeast mediated synthesis of silver nanoparticles." *International Journal of Nanoscience and Nanotechnology* 4, no. 1 (2008): 17-22.

22. Bhainsa, Kuber C., and S. F. D'souza. "Extracellular biosynthesis of silver nanoparticles using the fungus Aspergillus fumigatus." *Colloids and surfaces B: Biointerfaces* 47, no. 2 (2006): 160-164.

23. Roy, Ekta, Santanu Patra, Shubham Saha, Rashmi Madhuri, and Prashant K. Sharma. "Retracted Article: Shape-specific silver nanoparticles prepared by microwave-assisted green synthesis using pomegranate juice for bacterial inactivation and removal." *RSC Advances* 5, no. 116 (2015): 95433-95442.

CHAPTER 3

GENERAL CHARACTERIZATION TECHNIQUES

3.1. Structural characterization

3.1.1. X-ray Diffraction (XRD)

X-ray Diffraction is one of the most important techniques used for the determination of structural deformities in any sample. It is a rather simple and non- destructive classical method which has been used for structural analysis rather than studying its chemical composition as well as elemental content. From the seventeenth century onwards the scientific investigation of crystal symmetry and their uniformity in a particular sample has been carried out. It was Nicolas Steno, a Danish scientist that carried out the first study in crystal symmetry in 1669. And by 1784 Rene Just Hawy had made the conclusion regarding the geometry of each crystal face which paved way for a drastic change in existing crystallography. Later in 1893 it was William Hallowes Miller that introduced three small integers as labels for the unique identification of each crystal face. They were called as 'Miller Indices'. Till the end of nineteenth century, there were no valid conclusions regarding the various crystal structures. Later, in 1895, the discovery of X-ray by Wilhelm Rontgen led to the eventual development of X- ray crystallography. Since then numerous scientists have undertaken various studies on the wave nature of X-rays. By the beginning of twentieth century, William Henry Bragg had made arguments regarding its electromagnetic wave nature. In 1912, Max Von Laue discovered the behaviour of crystalline substance as three dimensional diffraction grating for X-ray wavelength. And thereby proved that X-rays are a form of electromagnetic radiation by observing that they undergo diffraction [1].

a) X-ray diffraction

A crystal has different lattice structures and lattice planes. When a light beam of suitable intensity comparable to the atomic spacing falls on the crystal planes, the beam gets scattered and re-radiated from different planes of the crystal lattice. If the rays are in phase and falling at an angle θ upon a set of symmetrically arranged planes with a spacing 'd', they will be constructively interfering and producing a diffraction pattern. This happens only when the path length difference between the rays ie., $2d \sin\theta$ is equal to the integral multiple of wavelength λ, of the incident beam [2][3].

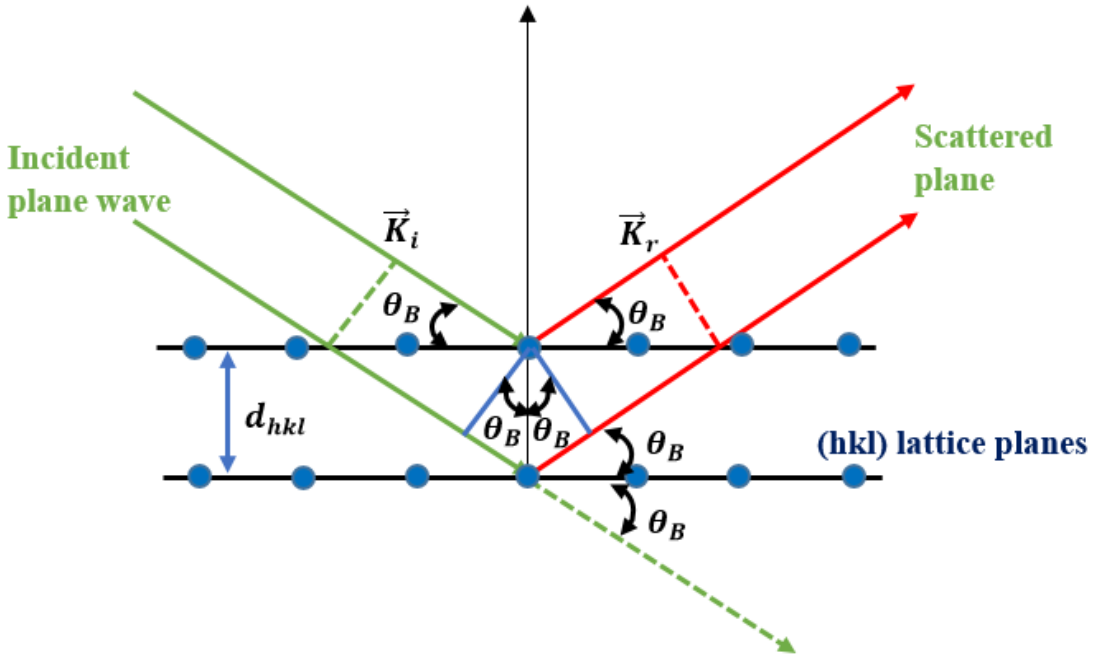

Figure 3.1.1.a: Schematic illustration of Bragg condition and Bragg's law

b) Bragg Equation

According to Bragg's law,

$$n\lambda = 2d_{hkl} \sin\theta_B$$

Where, n –integer which gives the order of diffraction

λ – the wavelength of the incident X-ray

d_{hkl} – the lattice spacing of (hkl) or inter-planar spacing

θ_B- the Bragg angle, the angle between the incident beam and lattice planes.

hkl – Miller indices

When $\sin\theta = 1, n\lambda = 2d$, that is the case of normal incidence.

The spacing, d can be calculated if we know the wavelength of the incident X-ray. For BCC (Body Centred Cubic Structure) and FCC (Face Centred Cubic Structure) crystals, atoms occupy the face rather than the corners and creates extra scattering centres [2][3]. The lattice constants are given by,

$$a = \frac{\lambda}{2} \frac{\sqrt{h^2 + k^2 + l^2}}{\sin\theta}$$

A graph between diffraction angle and diffracted X-ray intensity gives the XRD pattern. The sample scanned through an angle 2θ gives several peaks called as diffraction peaks. Each peak corresponds to a different order. The particle size can be determined from the 'd' value of each peaks. By comparing the obtained XRD pattern with the standard reference files (powder diffraction files (JCPDS)) we can easily identify the sample prepared as these files are unique for each element or compound.

c) XRD Instrumentation and working

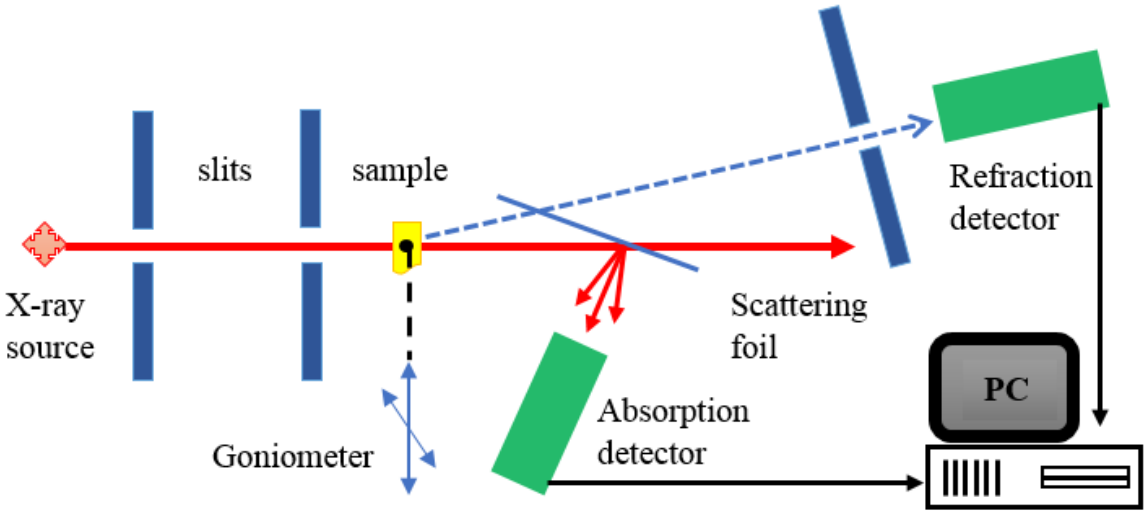

Figure 3.1.1.b: Schematic diagram of X-ray diffractometer

Generally speaking, using an X- ray diffractometer is not a new technique. It evolved 100 years ago and by now it has reached a much more refined form. Unlike earliest crystallographer, scientists can purchase the entire system or even can carry it as a portable unit. Normally, an X-ray diffractometer contains a source, Optics, a sample holder and a detector. The entire set up can be divided into two parts. The incident beam part which contains a source and a scanner while the diffracted beam part contains diffracted beam optics and detectors. The X-ray beam which emerges from the source is first passed through a collimator and then through a monochromator. There are of two types of monochromators, namely, crystal monochromator and filter monochromator (partially monochromatized).

The crystal monochromators are genrally made up of certain materials like sodium chloride, quartz etc., which reflects the incident beam suitably and splits it into the required wavelength [5][6]. The characteristic X-ray spectra has different components like K_α and K_β .

Here K_α is used for analytical purpose and K_β is filtered out. Once the beam is directed towards the sample, the sample holder will rotate the sample at angle of θ, while the detector will rotate at an angle of 2θ. This part is called a Goniometer. The obtained X-ray signals will get analysed by the detector and is then recorded on the PC attached to it [2][3].

A graph between diffraction angle 2θ and diffracted X-ray intensity gives the XRD pattern. Each peak corresponds to different order. The broadening of a peak is due to the deviation in crystallinity.

Using Debye Scherrer formula equation, the size of nano crystals can be estimated as,

$$D = \frac{K\lambda}{\beta \cos\theta}$$

where D is the crystallite size

K is the Scherrer constant

λ is the wavelength of incident X-ray

β is the full width half maximum (peak width)

2θ is the of angle of diffraction

3.1.2 Confocal Raman Microscopy

Raman spectroscopy is a non-destructive tool used for the characterization of samples. Confocal Raman spectroscopy is an improved version of Raman spectroscopy. It has same components as that of UV-Visible dispersing instrument and is often considered superior than infrared spectroscopy.

a) Instrumentation and working

Raman spectroscopy consists of mainly three components: a laser source, a specimen illumination system and a suitable spectrometer.

The Source is always made up of a laser with sufficient intensity to produce Raman scattering, since it is to be measured with a reasonable signal to noise ratio. Laser sources with blue and green region of spectrum have an advantage of producing necessary Raman scattering when compared with other laser sources.

Raman spectroscopy is often feasible with aqueous solutions, whereas infrared spectroscopy is severely limited due to the excessive absorbance of water [20]. Hence Raman spectroscopy can be used for the study of aqueous solutions, which is highly beneficial to the pharmaceutical industry. The sample holder in Raman spectroscopy can be an ordinary glass based material rather than crystalline halides as seen in other spectrometers. For liquid samples, a cuvette is used as sample holder. It can be made up of glass or quartz. While gas samples can be sealed in small capillary tubes.

Spectrometer which is used for the study of Raman spectrum should have large gathering power, must be provided with high resolving power prisms and a short focus camera.

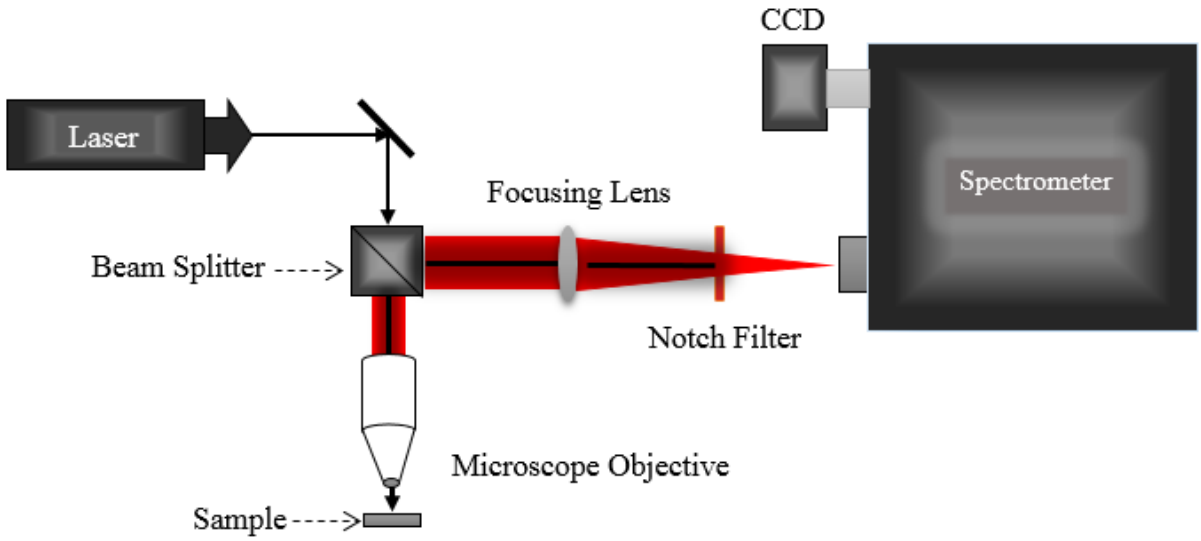

Figure 3.1.2: Schematic diagram of Microscopic Raman spectroscopy [14]

b) Sample analysis

The light from the laser source is allowed to fall on the specimen and get scattered which is focussed by the entrance slit. Then it is allowed to pass through the analyser prism and finally through the monochromator. The radiations observed in Raman Spectra are of three types: The Stokes line, the anti-stokes line and Rayleigh line. A chopper is used in between to respond only to the Rayleigh line. Thus by rejecting intense Rayleigh scattering, it makes it possible to detect the weak Raman shift in components. Since the Stokes lines are more intense than the corresponding anti-Stokes lines, this part of spectrum is used for the analysis. The

magnitude of Raman shifts is independent of the excitation wavelength, as it is directly related to the vibrational energy modes of the analyte molecules. Thus Raman Spectroscopy is a potentially useful source for the study of structure, composition and stability of coordination compound.

- **SERS (Surface-Enhanced Raman Spectroscopy)**

Surface enhanced Raman spectroscopy functions in the same way as that of ordinary Raman spectroscopy. The only difference is that, in SERS, the magnitude of Raman depends upon the wavelength absorbed by the colloidal metal particles like silver, gold or copper on the surface of the sample. Prior research has shown that the resultant Raman lines may be enhanced by a factor of 10^3 to 10^6. [15]

3.2 Optical Characterization

3.2.1 UV-Visible absorption spectrophotometry

Ultra violet – visible absorption spectroscopy is one of the widely used refined optical spectroscopy methods in the field of science. It is used for quality checking , drug identification, bacterial detection, dye sensitization etc. Here, energy of the absorbed light promote or excite the electrons which are occupied in different bonding environment within the sample. Since each bond has different strength, corresponding ionization energy will be different. As shorter wavelength carries more amount of energy than the longer wavelength, their absorption range will also change. The relation connecting the frequency of light absorbed and energy is given as,

$$E = h\upsilon$$

Where E is the energy, h is the Planck's constant and υ is the frequency of the photon.

The advantage in UV- Visible spectroscopy is that the electrons with different bonding strength will absorb different amount of energy which will result in varying absorption peaks. Which in turn is useful for the analysis of different substance by specifying the maximum absorbance corresponding to the wavelength.

a) Instrumentation and working

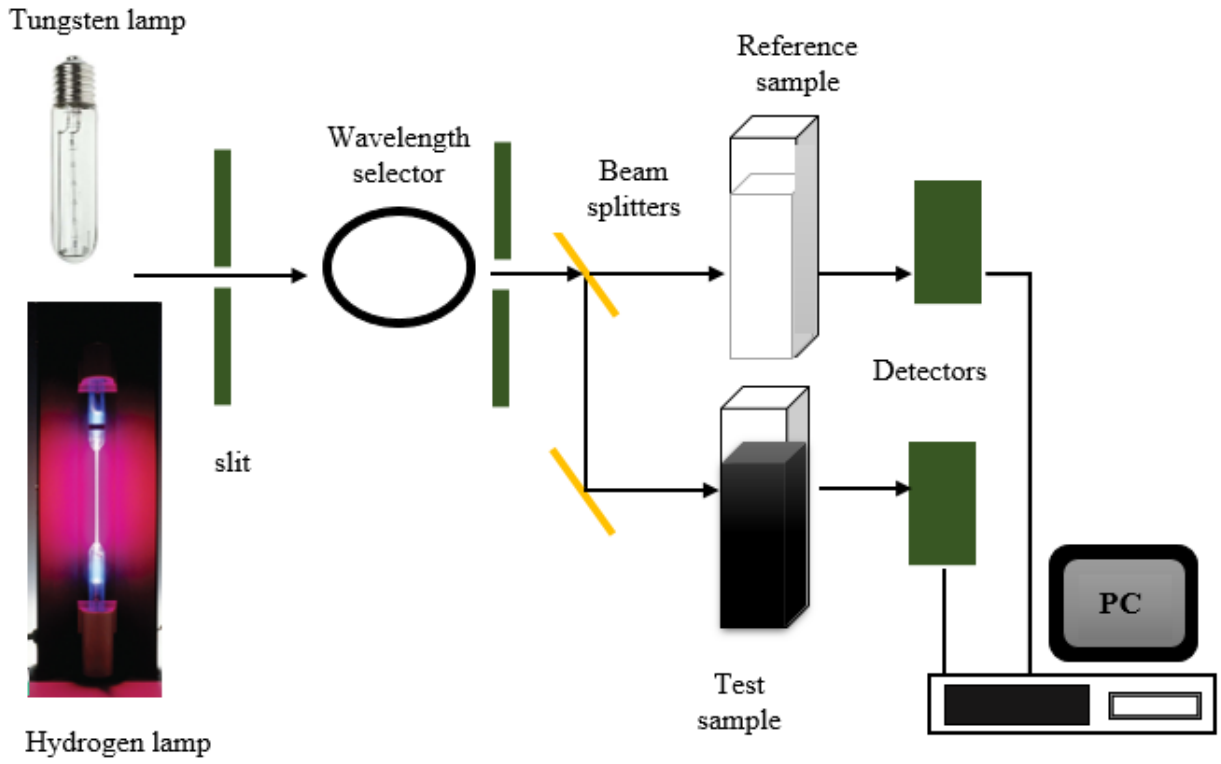

Figure 3.3: Schematic representation of UV-Visible spectrophotometry

The spectroscopy deals with the interaction of light with matter. There is single beam spectroscopy as well as double beam spectroscopy. Ultra violet – visible absorption spectroscopy consists of a light source, wavelength selector, beam splitter (as it is double beam spectroscopy), sample holder (cuvettes for liquid samples), a detector (can be a photocell or photo diode) and a personal computer for signal processing.

It uses two lamps as the light source; one which supply visible light whose wavelength ranges from 400 nm to 700nm and other is ultraviolet light whose wavelength ranges from 200 nm to 400 nm approximately. The beam passes through the monochromator, so that only a particular wavelength will be allowed at a time from a range of wavelengths for further characterization. This monochromatic light then gets transmitted through a beam splitter. The function of the beam splitter is to split the intensity of light into two equal halves. One of them passes through the test sample while the other passes through the blank sample (reference liquid). The reference liquid does not absorb any wavelength. As it transmits all the wavelengths (entire incident beam I_0), its absorbance is taken to be 0 [3][10]. But the test sample will absorb some amount of light at a particular wavelength. Hence the transmission is not 100% and the intensity of emerged light should be less than incident beam I_0. These intensities

are then detected by the detectors and are get recorded by the system connected to them. They will display the absorption spectrograph corresponding to the sample placed [3][10][11].

b) Sample analysis

The output obtained from the detector gets recorded and processed by the personal computer connected to the spectrometer. Whenever the light passes through the blank sample, it will pass through the test sample as well. If the sample does not absorb light at that particular wavelength, then the transmittance become 100% or $I = I_0$.

Consider the Beer-Lambert law,

$$A = \log \frac{I_0}{I}$$

Where A is the absorbance

I_0 is the intensity of monochromatic light

I is the intensity of transmitted light

i) When $I = I_0$, then $A = 0$

ii) When $I < I_0$, then $A > 0$

3.3 Morphological characterization

3.3.1 Scanning Electron Microscope (SEM)

Scanning Electron Microscope (SEM), is an electron microscope, which can provide high resolution images. This characterization technique can be used for the determination of surface morphology of the samples. It was in 1937 that Manfred von Ardenne suggested the theory of SEM in comparison with TEM (Transmission Electron Microscope) [12].

a) Instrumentation and working

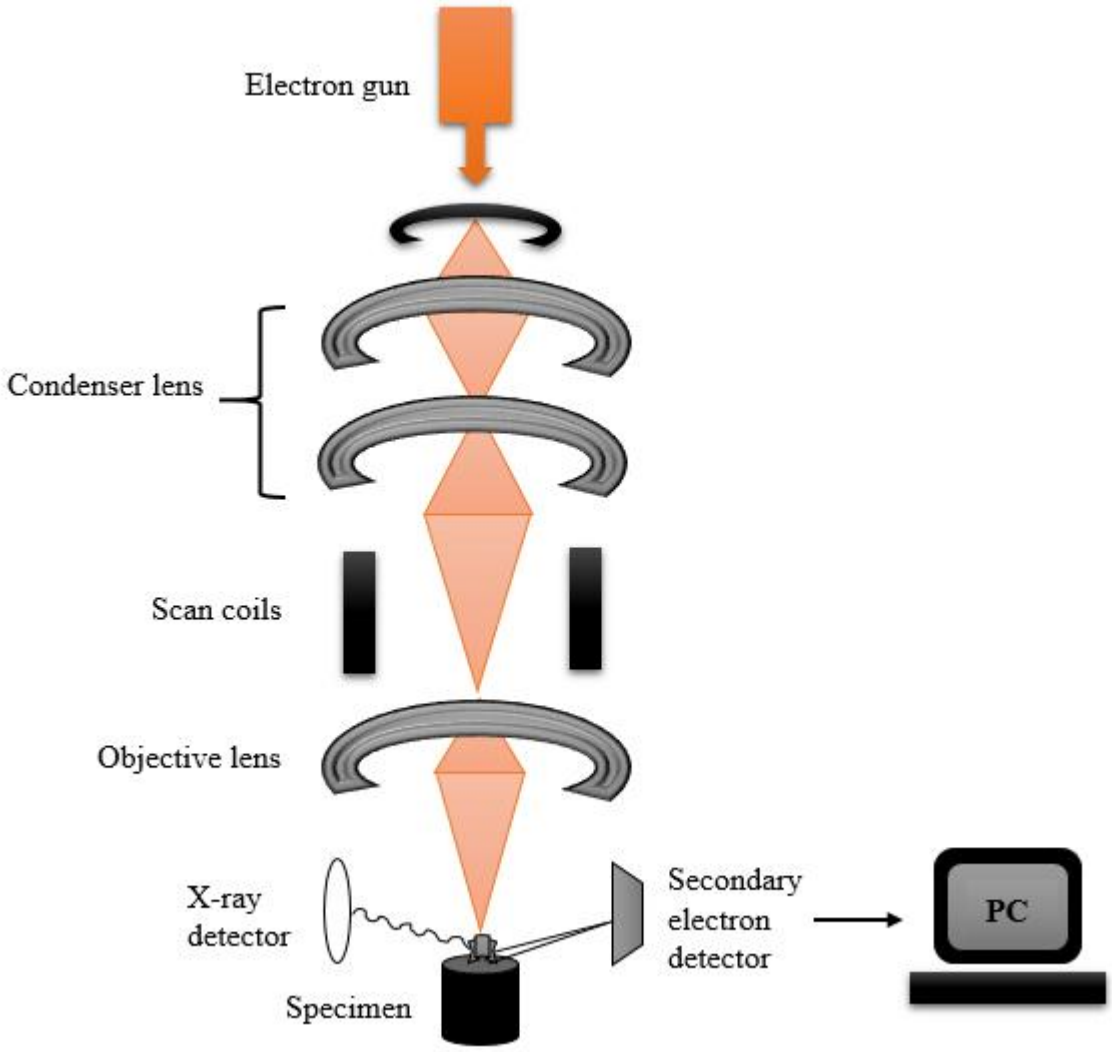

Figure 3.4: Schematic diagram of SEM [2]

A Scanning Electron Microscope consisting of an electron gun, two condenser lenses (called as first condenser lens and second condenser lens), an objective lens, detectors and deflection coils.

The electron gun is used to eject a beam of electrons. The emission of electron beam is made possible by heating a cathode, usually tungsten to a high temperature and by allowing these electrons to flow to the anode (metal plates). Such electron guns are thermionic in nature. Other types like upgraded or field emission guns and Schottky guns are also preferred in SEM [13].

Magnification in SEM images can be made using the lens. This can be controlled by changing the strength of the lens. A rotationally symmetric magnetic field is created when the current passes through the wire which is wounded over the coils. The condenser lens can focus the electron beam and direct it to the objective lens. The objective lens focuses the electron beam to the sample kept at the bottom.

The deflection coil (or scanning coil) helps scan the sample. Two sets of coils are used for raster scanning done over the specimen. The electron beam then reaches the sample taken in the sample holder. The sample can be tilted or rotated and fixed in the field of view. There are two electron detectors: one is for secondary electrons and the other is for back scattered electrons. The secondary electrons are collected by electrically attracting them towards a scintillator and then to a photomultiplier. The amplified analogue signals are then converted to a digital from. In a similar way there is a detector for back scattered electron. Both are recorded and the final resultant SEM image is displayed on the personal computer attached to it.

b) Sample analysis

When electron beam interacts with sample or specimen, different types of signals are produced [13]. Some of the signals are produced by the interaction of electrons with the sample surface; since some of the electrons can only escape from the few nanometer thick surface layer. These electrons are called as secondary electrons (SEs). The another category of electrons called back scattered electrons arises due to elastic scattering, which gets reflected from the sample [12].

Secondary electrons are so called because when the electron beam is incident on the sample, the primary radiation will generate some ions, photons or electrons with high energy as an ionisation product. They are produced from the inelastic scattering of electron beam. The emission of valance electron usually keeps the energy of these secondary electrons to a minimum amount. The photoelectrons produced with high energy (>50 eV) are considered to be primary radiation.

Back scattered electrons are generated due to the elastic scattering of incident beam of electrons. These are higher energy electrons which are ejected from the depth unlike the secondary electrons which originated from layers which are a few nano meters deep on the sample surface. As the intensity of these back scattered electron are higher at that particular areas, it can be used to identify the surface irregularities and presence of heavier atoms etc. on the sample surface.

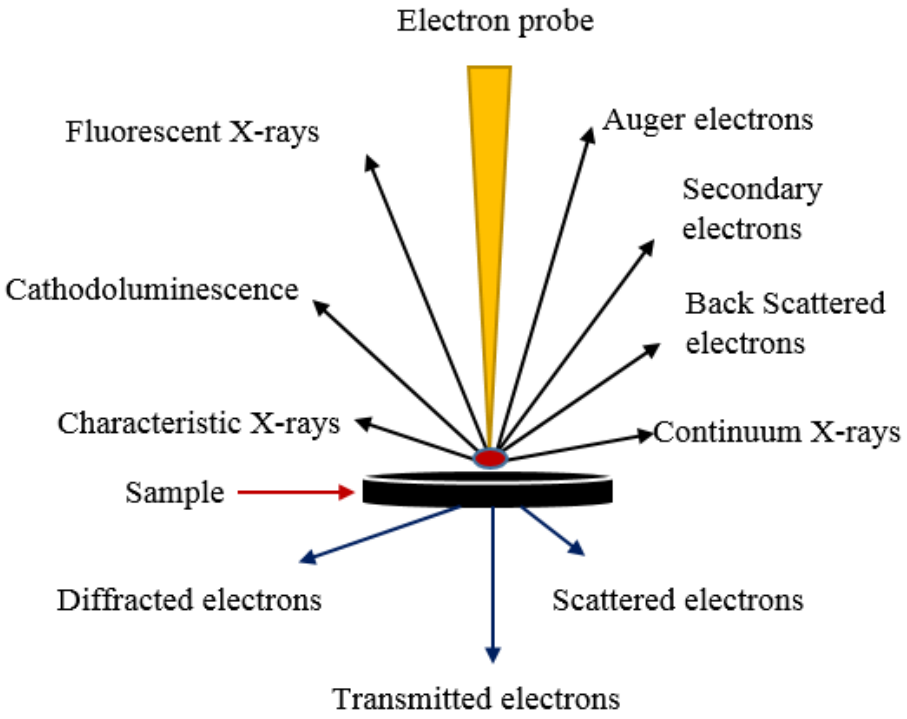

Figure 3.5: Various interaction processes inside a sample

Characteristic X-rays are produced when electron beam interacts with the inner shell electrons. As the electrons get excited and leave, the outer shell electrons (higher energy electrons) fill the spaces. This released energy causes characteristic X-rays.

- **FE-SEM (Field Emission Scanning Electron Microscope)**

Field emission scanning electron microscope (FE-SEM) is an advanced form of SEM imaging. Here the analyte gets disturbed by the incoming beam and causes the emission of secondary electrons and back scattered electrons. This is usually carried out at high vacuum and low voltage [18]. High quality images are obtained due to the slight electrical charging of the sample.

3.3.2 Transmission Electron Microscope (TEM)

Transmission electron microscope (TEM) is another technique used for morphological characterization. It uses a very high energy electron beam for scanning the specimen. TEM images can be modified either into a STEM (Scanning Transmission electron microscope) or a HRTEM (High Resolution Transmission electron microscope) image, depending upon the resolution obtained [2].

a) Sample analysis

TEM analysis can be done in the same way as that of SEM analysis. The only difference is that, instead of back scatted electrons and secondary electrons it uses the transmitted electrons for collecting information about the sample.

There are two modes of imaging: Bright field imaging and Dark field imaging [2]. When the electron beam falls on the specimen, it allows the beam to get transmitted through it and then directs it to the imaging system. Here the imaging system can be a Phosphor screen or any other fluorescent or light sensitive plate. The flow of these electrons are adjusted by condenser and objective lenses. The objective lens allows the direct beam to pass and contains a plate where the scattering of electrons occur. It then focus on a back focal plane. So obtained images are called bright field images. Whereas, if the direct beam is obstructed and only diffracted beam is transferred to the back focal plane, it produces a dark filed image. This type of image can give the idea about crystal orientations as well [2].

b) Instrumentation and working

TEM consists of several components which include electron gun, condenser lenses, objective lenses, light sensitive sensor, sample grid and a project lens. The working principle behind all modified TEM versions are the same with differences in its image quality.

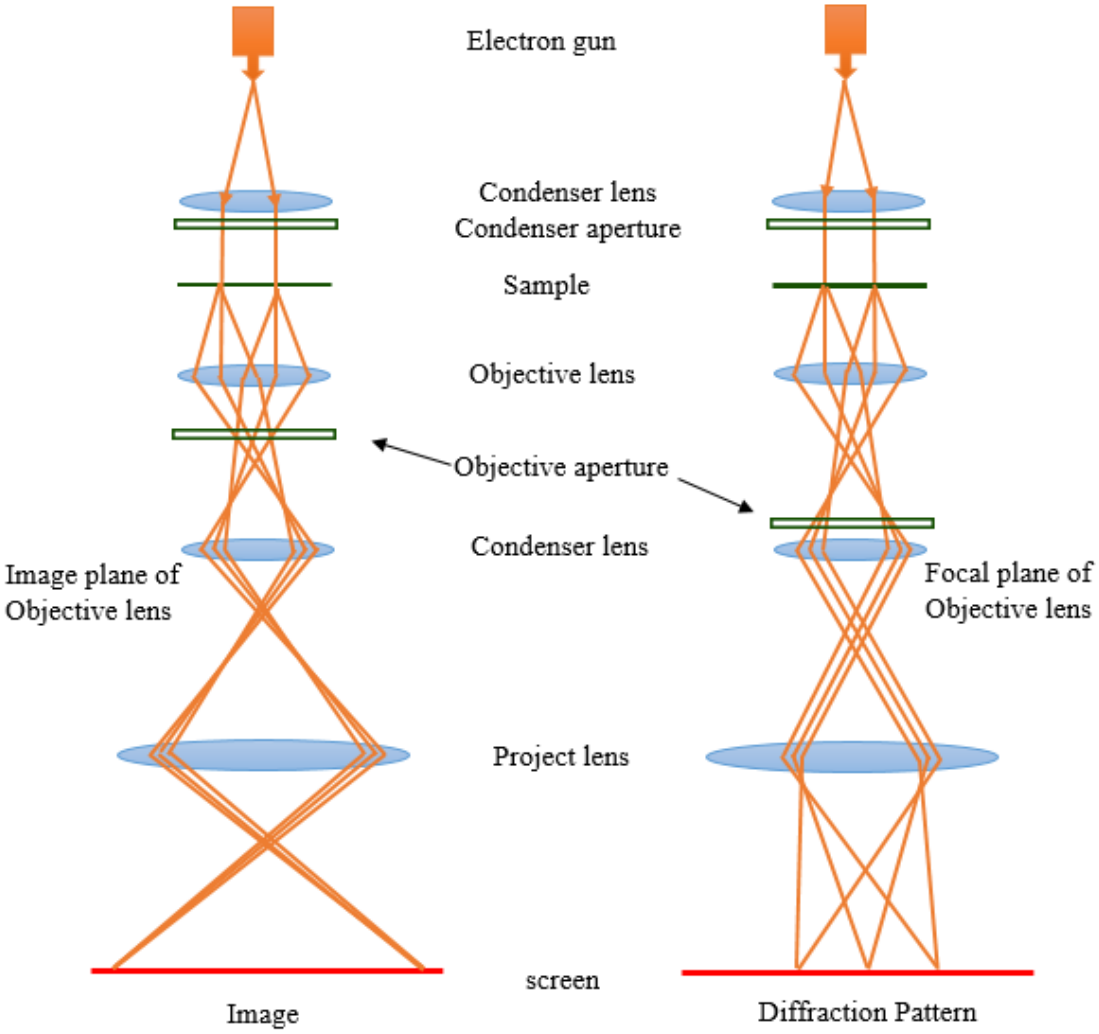

Figure 3.6: Schematic diagram of two TEM imaging

REFERENCE

1. San Román, Leandro Sequeiros. "Primera traducción completa en castellano del" Prodomus"(1669) de Nicolás Steno (1638-1686)." Llull: Revista de la Sociedad Española de Historia de las Ciencias y de las Técnicas 27, no. 58 (2004): 191-194.

2. Friedrich W, Knipping P, von Laue M (1912). "Interferenz-Erscheinungen bei Rontgenstraheln". Sitzungsberichte der Mathematisch-Physikalischen Classe der Koniglich-Bayerischen Akademie der Wissenschaften zu Munchen. 1912:303

3. Santhi A, The Nanoscope: An Introduction to Nanoscience and Nanophotonics, Medtech, 2016

4. P.K Ghosh, M K Mitra and K K Chattopadhyay, /Vanofec/0/.16,107,2005

5. Yougui Liao, Practical Electron Microscopy and Database,3882, 2006, www.globalsino.com/EM/

6. B.K Sharma, "Instrumental methods of chemical analysis", 17th edition, 1997-1998, GOEL publishing house. Page 329-359

7. Dougles, A skoog, F James holles, Timonthy A, "Principles of instrumental analysis", 5th edition, 277-298

8. Gurudeep R, Chatwal, Sham k anand, "Instrumental methods of chemical analysis", 2.303-2.332

9. Wikipedia contributors, "X-ray crystallography," Wikipedia, The Free Encyclopedia, https://en.wikipedia.org/w/index.php?title=Xray_crystallography&oldid=1101201624 (accessed July 18, 2022)

10. Preston, Colin, Yunlu Xu, Xiaogang Han, Jeremy N. Munday, and Liangbing Hu. "Optical haze of transparent and conductive silver nanowire films." Nano Research 6, no. 7 (2013): 461-468.

11. Kumar, Subodh. "Spectroscopy of organic compounds." 2008.

12. Primer, A. "Fundamentals of UV-visible spectroscopy." Copyright Hewlett-Packard Company, Hewlett-Packard publication 12-5965 (1996).

13. Von Ardene, Manfred, "Improvements in electron microscopes", published 1939-08-15

14. Scanning Electron Microscope A to Z-Basic Knowledge for using the SEM, JEOL Serving advanced Technology [https://www.jeol.co.jp/en/applications/pdf/sm/sem_atoz_all.pdf]

15. Gurudeep R Chatwal, Sham K Anand, Instrumental methods of chemical analysis, 2013, 2.83-2.101

16. Silverstein, M, Robert., Webster, X, Francis., Kiemle, D., "Spectrometric Identification of Organic Compounds", John Wiley & Sons, 7 edition

17. Gurdeep, R., Sham Chatwal, and K. Anand. Instrumental methods of chemical analysis. Himalaya publishing house, 2016.

18. Jaya, Ramadhansyah Putra. "Porous concrete pavement containing nanosilica from black rice husk ash." In New Materials in Civil Engineering, pp. 493-527. Butterworth-Heinemann, 2020.

19. Mayeen, Anshida, Leyana K. Shaji, Anju K. Nair, and Nandakumar Kalarikkal. "Morphological characterization of nanomaterials." In Characterization of Nanomaterials, pp. 335-364. Woodhead Publishing, 2018.

20. Tranter, George E., and Delphine D. Le Pevelen. "Chiroptical spectroscopy and the validation of crystal structure stereochemical assignments." *Tetrahedron: Asymmetry* 28, no. 10 (2017): 1192-1198.

CHAPTER – 4

SYNTHESIS AND ANALYSIS

I. PREPARATION METHOD

The synthesis of graphene oxide (GO) constitutes the first part of this project. After the successful preparation of graphene oxide, the fabrication of reduced graphene oxide- silver (rGO/Ag) nanocomposites was done.

4.1 Preparation of Graphene oxide

Graphene oxide nanoparticles were synthesised using "Modified Hummer's method of synthesis" [1]. The chemical reaction involved here can be depicted as shown below:

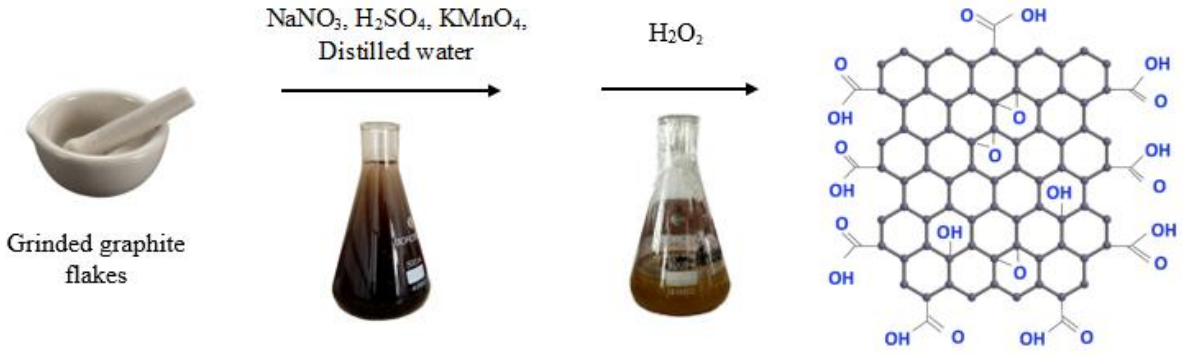

Figure 4.1: The schematic representation of synthesis of graphene oxide.

Materials and apparatus required:

Graphite flakes- was purchased from Sigma Aldrich, whereas, Sodium nitrate ($NaNO_3$), Sulphuric acid (H_2SO_4), Potassium permanganate ($KMnO_4$), Distilled water and Hydrogen Peroxide were all purchased from Nice chemicals (P) LTD. And finally Hydrochloric acid (HCl)- was purchased from Merck life science Private Limited.

Procedure:

Graphene oxide was synthesised via oxidation and exfoliation of 3 dimensional graphite sheets. The synthesis part was carried out with reference to Paulchamy, Balaiah, G.

Arthi,et.al [1]. 2g of Graphite flakes and 2g of $NaNO_3$ were mixed in 90 ml of H_2SO_4 (97%) in a conical flask which was kept under ice bath (of temperature 0^o to 5^oC) with continuous stirring. The mixture was stirred for 4 hours and 12 g $KMnO_4$ was added to the suspension in a slow pace. The rate of addition was carefully controlled so as to keep the reaction temperature lower than 15^oC. The mixture was then diluted with distilled water and stirred for 1.15 hours after which the ice bath was removed. The mixture was then once again stirred at 35^oC for 1.15 hours. It was then kept in reflux system at 98^oC for 20 minutes. 40 ml of H_2O_2 was then added and the temperature was brought down to 25 ^oC while continuously stirring it for2 hours. The as prepared solution was then added to 400 ml of water taken in a beaker and stirred for 1 hour. It was then kept aside for 24 hours. The resulting mixture was repeatedly washed with HCl and followed by distilled water. The resultant precipitate was dried at 60^oC for more than 10 hours to obtain GO powder.

4.2 Preparation of reduced graphene oxide/ silver nano (rGO/Ag) composite

The synthesis of reduced Graphene oxide- silver nanoparticles was done by solvothermal synthesis method. According to Quocanh N. Luu, Joshua M. Doorn,et.al in order to prepare various low dimensional inorganic materials having different morphologies, the hydrothermal or solvothermal synthesis method is more convenient [2].

The chemical reaction involved is as follows:

$$AgNO_3 + NaCl + PVP \rightarrow Ag + NaNO_3 + C_6H_9Cl + NO\uparrow$$

Materials required:

Silver nitrate (AgNO3), Ethylene glycol (EG), Sodium chloride (NaCl), Isopropyl Alcohol (IPA), and Acetone which was purchased from Nice chemicals (P) LTD, and Polyvinylpyrrolidone K30 (40000 MW)- bought from Loba chemie Pvt. Ltd.

Procedure:

Reduced graphene oxide -Silver nanowire can be synthesised using solvothermal method [2]. To begin with, 0.34 g of $AgNO_3$ was dissolved in 30 ml of ethylene glycol. This was followed by dissolving 0.883 g PVP and 2.3 g NaCl in 20 ml ethylene glycol at 120^oC while stirring at 600 ppm. Then the PVP, NaCl, Eg solution was added to the $AgNO_3$/EG

solution drop by drop under vigorous stirring. After it was allowed to mix for 5 minutes, it was transferred into a100 ml autoclave. The autoclave was then heated at 160^{o}C for 7 hours and allowed to cool at room temperature. The resultant was washed 3 times with isopropanol, and centrifuged with acetone at 5000 rpm to get the precipitate.

The obtained sample was filtered using Whatman grade 1 filter paper. It was then dried in the oven at 160^{o}C for 4 hours after which it was ground it into fine powder using a mortar.

4.3 Fabrication of rGO/Ag substrate

The preparation of rGO/Ag substrate for the SERS application is a simple process.

Procedure:

0.01 g of rGO/Ag powder was weighed and added to 1 ml of ethylene glycol solution which was then sonicated using a digital Ultrasonic cleaner for 3 hours. 10 microliter of as prepared rGO/Ag solution in ethylene glycol was pipetted out on a cleaned glass slide/silicon wafer. Once it was dried in the oven for one hour at 50^{o}C, a film was successfully obtained over the slide/wafer. The procedure was repeated until a desired thickness of the substrate was obtained.

4.4 Preparation of rGO/Ag substrate for dye detection and pesticide sensing

The project was aimed at testing the efficiency of detecting certain dyes and chemicals using the rGO/Ag nanocomposite substrate prepared. While, chemical dye Crystal violet was used for dye detection, thiram (sodium diethyldithiocarbamate) was used for pesticide detection. Crystal violet solutions with different molar concentrations, ranging from 10^{-2} M to 10^{-11} M were prepared by series dilution method. Whereas, the bulk thiram was dissolved in isopropyl alcohol under vigorous stirring to obtain solutions of different concentrations ranging from10^{-5}M to 10^{-8}M.

4.5 Preparation of well for antibacterial action

The antibacterial test was done using well diffusion method in which the mean inhibition zone seen on disks prepared is measured.

Materials required:

While Agar agar and bacteriological nutrient broth were purchased from Nice chemicals (P) LTD, Petri plates, Cotton swabs, Tetracycline (TE) 30 mcg susceptibility and Test discs were purchased from HiMedia Laboratories Pvt. Ltd.

Procedure:

In order to check the efficiency of the prepared sample of rGO/Ag nanocomposites towards bacterial actions it was tested against two bacterial strains: Escherichia-coli (E. coli) and Staphylococcus-aureus (S. aureus) [3].

The inhibition was studied from the petri plates created using nutrient Broth and Agar agar bacteriological powder, which is capable of supporting the growth of these organisms. The bacteria were inoculated from a pure culture and were grown for 24 hours at 29^{o}C. A media was prepared by dissolving 1.3g of the nutrient broth and 2g of agar agar in 100ml distilled water. Then it was autoclaved at 100^{o}C and kept under UV light for 30 minutes. The plates were seeded with the inoculum (E. coli and S. aureus) using sterile cotton swabs. Using a steel borer of 8 mm, a well was created in each of the two petri dishes. Each of them were then further divided into two equal parts where the portion with the well was labelled as ‘rGO/Ag’ and the other was labelled as ‘control’. Both the setups were then placed in the incubator 24 hours at 30 ^{o}C. The rGO/Ag solution prepared was then poured into the wells and the changes were studied and recorded

II. ANALYSIS

The material properties including the structural, optical and morphological nature of the prepared rGO/Ag nano composites were analysed. The results obtained is presented and identified in this chapter.

4.6 Graphene Oxide (GO)

4.6.1 X-Ray diffraction analysis of GO

The structural characterization of GO was done using X-ray diffraction technique. The X-ray diffraction pattern gives the information about different crystalline planes present in the prepared sample.

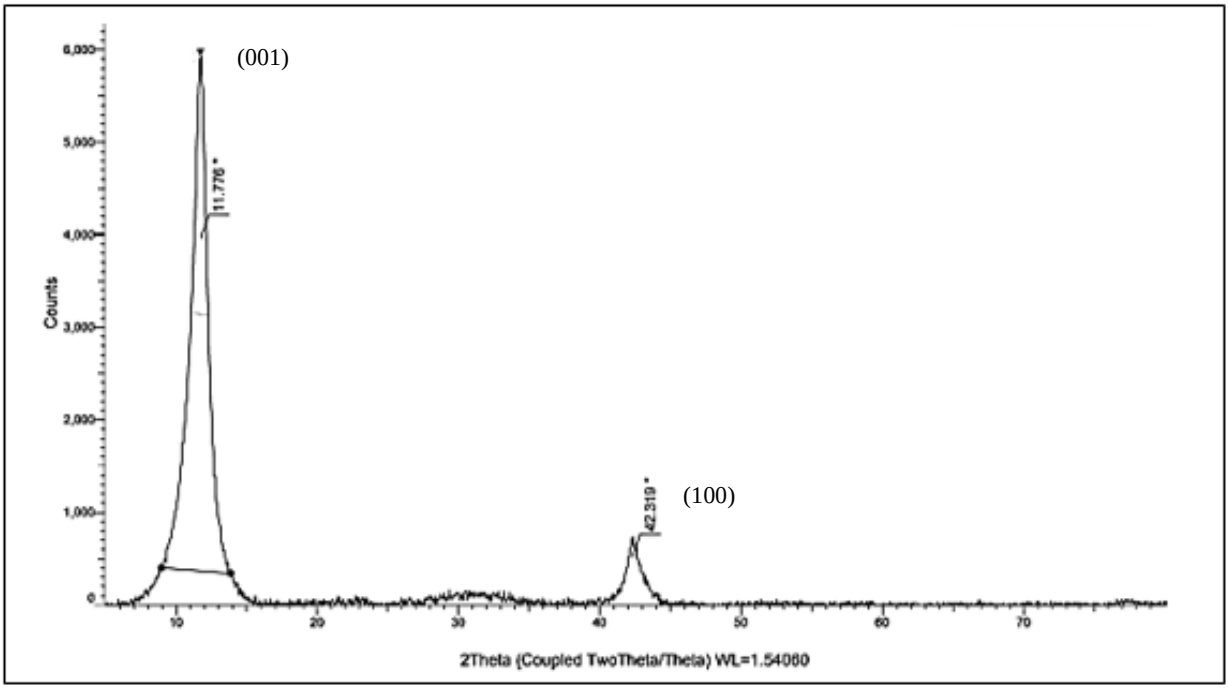

Figure 4.6.1.a: Powdered X-Ray Diffraction pattern of graphene oxide

Figure 4.6.1.a depicts the powdered X-ray diffraction pattern of Graphene Oxide. The PXRD pattern of GO exhibits a strong 2θ = 11.776° (with (d) spacing of 7.508 Å) peak value that corresponds to the plane (001). This indicates a complete oxidation and exfoliation of graphite flakes precursor. Additionally, a small peak at 2θ = 42.319° (with the (d) spacing of 2.134 Å) was observed, corresponding to the (100) plane. The reflection from major graphite planes (002) and (004) are not observed which leads to the conclusion that a typical crystal

graphite structure is absent. In GO, the interlayer spacing increased as compared to graphite due to addition of oxygen-containing functional groups during oxidation of graphite. Also there is no obvious characteristic peaks of impurities in the pattern [8][9].

4.6.2 UV-Visible analysis of GO

Optical characterization was done via UV-Visible absorption spectrometer.

The result obtained from UV absorption analysis is shown in Figure 4.6.2. For graphene oxide two characteristic peaks are observed. The peak at 235 nm is due to $\pi \rightarrow \pi^*$ transition of aromatic C=C bond while the other peak seen at 297 nm is due to $n \rightarrow \pi^*$ transition of C=O bond [10].

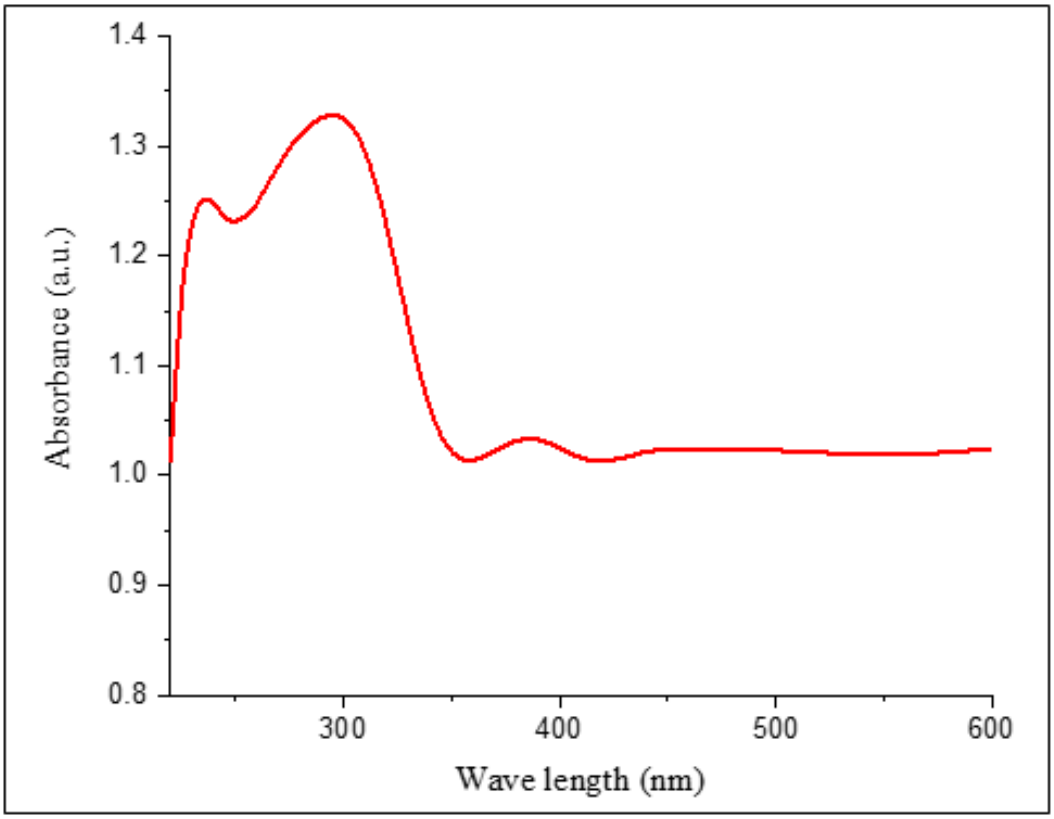

Figure 4.6.2: UV-Vis absorption spectrum of GO

4.6.3 SEM analysis of GO

The morphological analysis of GO nanoparticles was done by Scanning electron microscope.

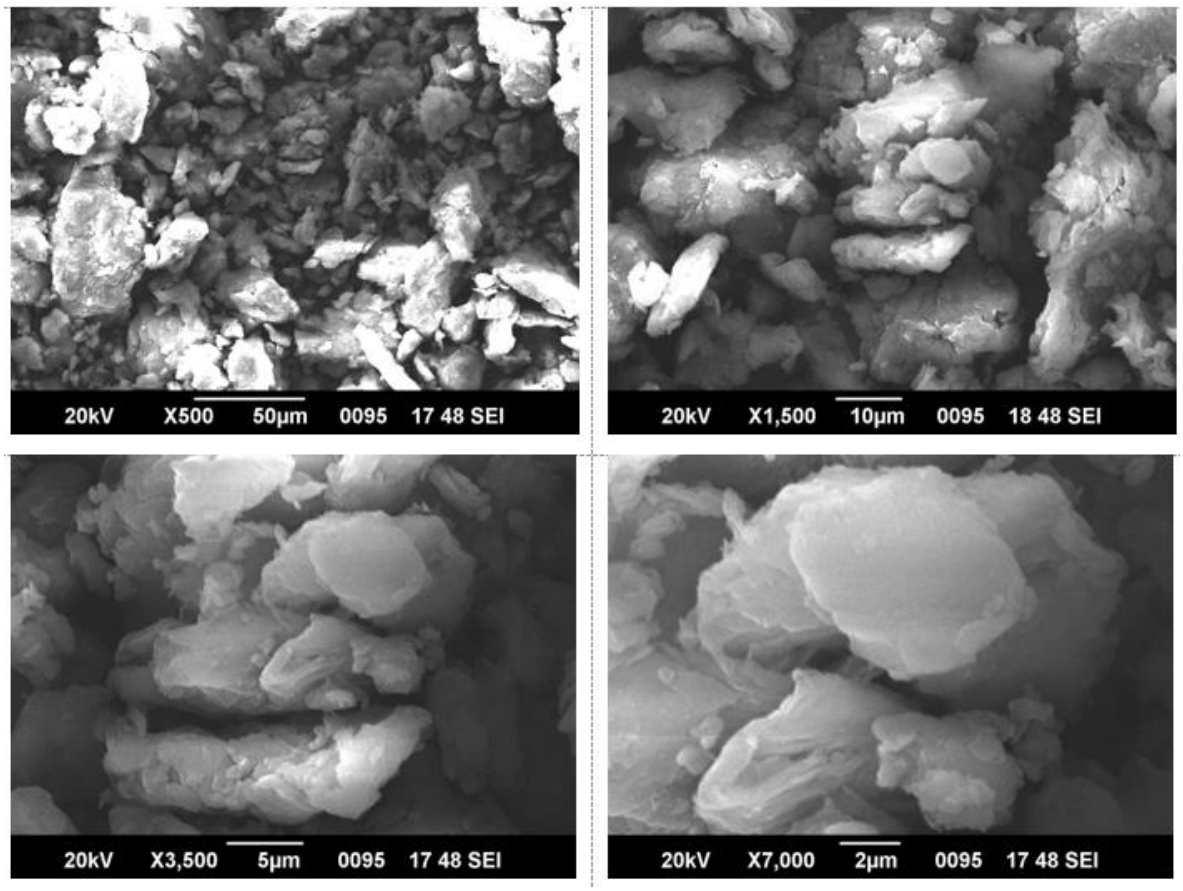

Figure 4.6.3.a: SEM images of GO

Figure 4.6.3.a gives the morphology of sample GO examined by SEM and confirms the formation of GO sheets in the prepared specimen. The Field emission scanning electron microscopy (FE-SEM) image of GO sheets shows a flake like morphology. It can be seen in the figure 4.6.3.b.

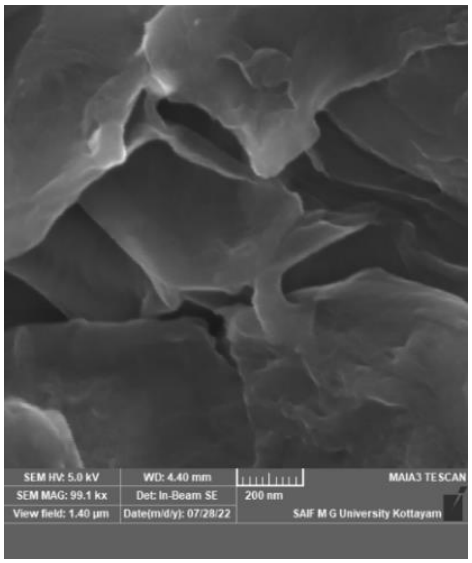

Figure 4.6.3.b: FE-SEM image of GO

4.6.4 Raman analysis of GO

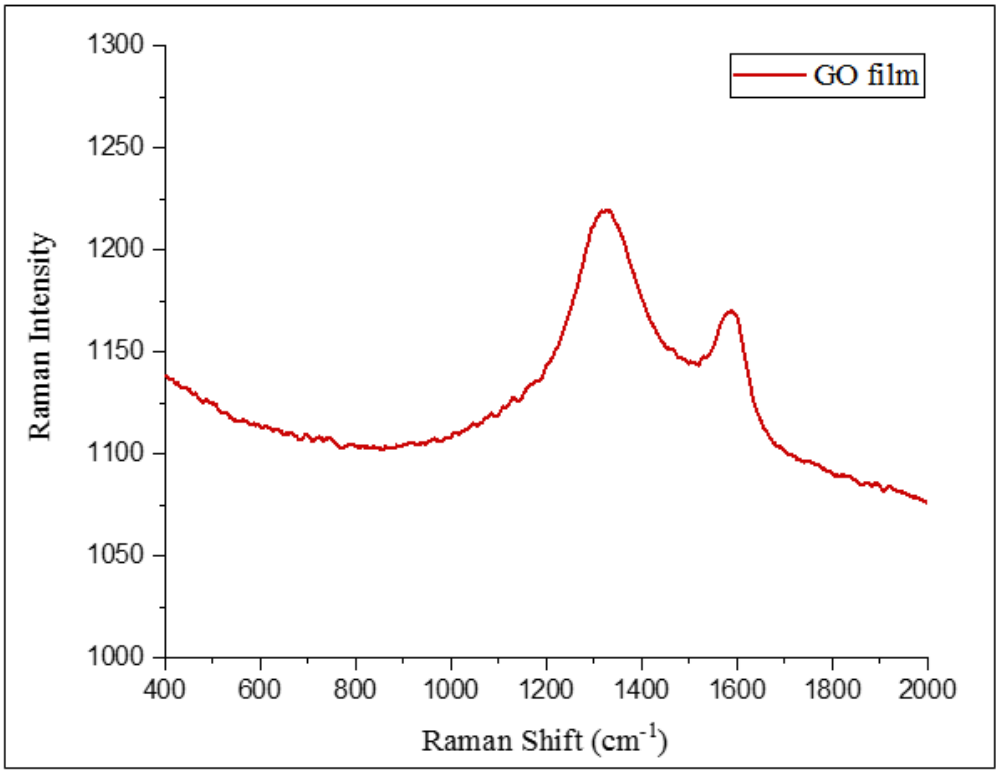

Figure 4.6.4: Raman spectrum of GO

Figure 4.6.4 illustrates the Raman spectra of GO with two bands in vibrational modes. One at 1321 cm^{-1} called D band, attributed to K-point phonons of A_{1g} symmetry and the other at 1581 cm^{-1}, called G band, attributed to zone- center phonons of E_{2g} symmetry[1,2][11]. A_{1g} vibrational modes are due to the lack of translational symmetry and are active only along the edges of GO sheets. Here the I_D/I_G ratio is calculated as 1.04 [16].

4.7 Reduced Graphene Oxide/Silver nano composite

4.7.1 X-Ray diffraction analysis of rGO/Ag nano composite

The structural characterization of rGO/Ag nanocomposites was done using X-ray diffraction technique. The XRD pattern gives the information about different crystalline planes present in the prepared sample.

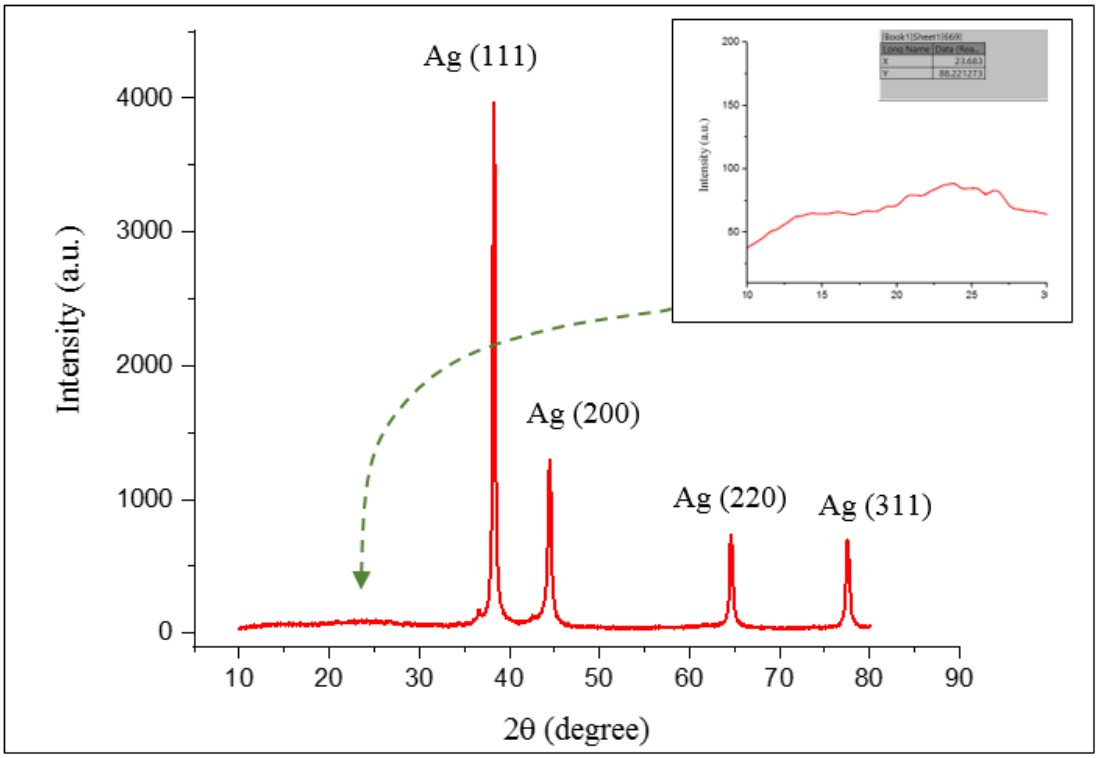

Figure 4.7.1: Powdered X-ray diffraction pattern of rGO/Ag nano composite; inset: unoxidized GO peak at 23.7°

The X-ray diffraction of rGO/Ag nanomaterial reveals that the peaks observed at 38.280°, 44.466°, 64.595° and 77.523° are due to the reflection from (111), (200), (220) and (311) planes of AgNPs. While the broadened peak at 23.7° is due to graphene oxide, corresponding to the plane (002), which indicates the reduction of GO [17]. Using the peak positions, the calculated d spacing is 2.349 Å for rGO/Ag, whereas d_{002} of graphite is .335 nm [10].

- **Particle size determination**

The particle size of a nanoparticle, D can be calculated using Debye-Scherrer equation:

$$Particle\ size, D = \frac{K\lambda}{B\cos\theta}$$

Where K is a constant which is nearly equal to 0.94

B is the full width half maximum measured in radian

λ is the wavelength of X- ray = 1.54060 x 10^{-10} m

2θ (in degree)	θ (in degree)	θ (in radian)	B (degree)	B (radian)	Particle size D (nm)
38.283°	19.1415°	0.3339	0.314	0.005477	26.441
44.467°	22.2335°	0.3878	0.376	0.006559	22.079

Hence average particle size, D = 24.26 nm

4.7.2 UV-Visible analysis of rGO/Ag nano composite

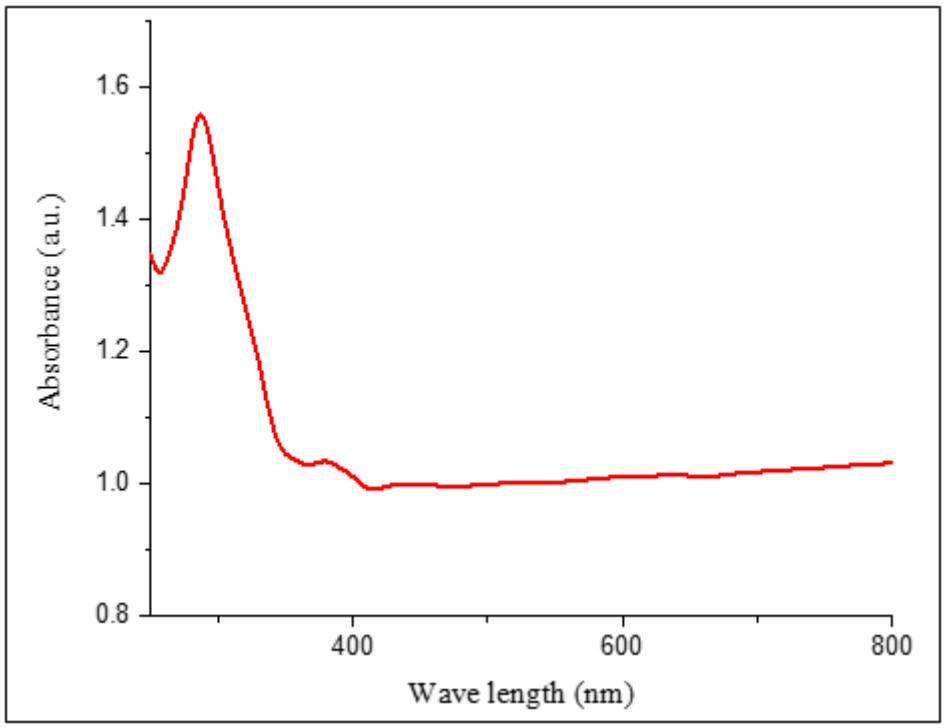

Figure 4.7.2: UV-Vis absorption spectra of rGO/Ag

In addition to the peak observed at 287 nm, which is due to the presence of rGO, a new absorption peak is observed at 379 nm. This peak is due to the presence of silver nano particles which indicates the deposition of silver nano particles on the GO sheets [18].

4.7.3 SEM analysis of rGO/Ag nano composite

The morphological analysis of rGO/Ag nanoparticles was done by SEM analysis. SEM-EDX image of rGO/Ag is given in the figure below. Fig.4.7.3.a gives data about the elemental content in it.

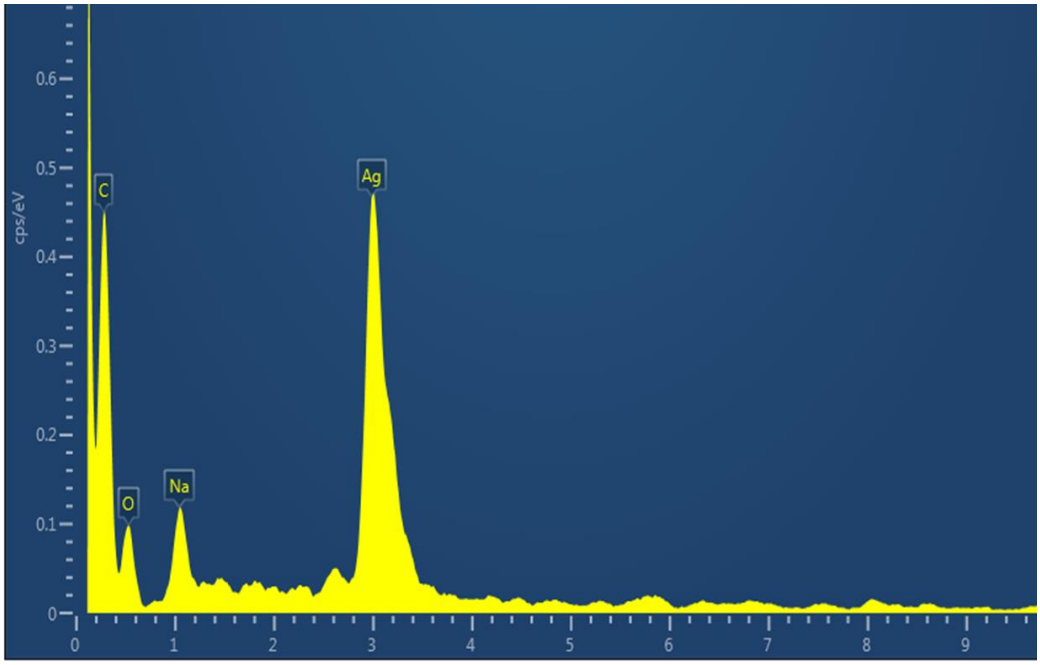

Figure 4.7.3.a: SEM-EDX of rGO/Ag

The EDX spectrum of the composite in the figure 4.7.3.a confirms the presence of Ag nanoparticles and the high intensity peak corresponds to carbon while another appreciable peak of oxygen atom confirms the presence of GO.

FE-SEM images of rGO/Ag nanoparticles is given in figure 4.7.3.b. It confirms the results of XRD analysis.

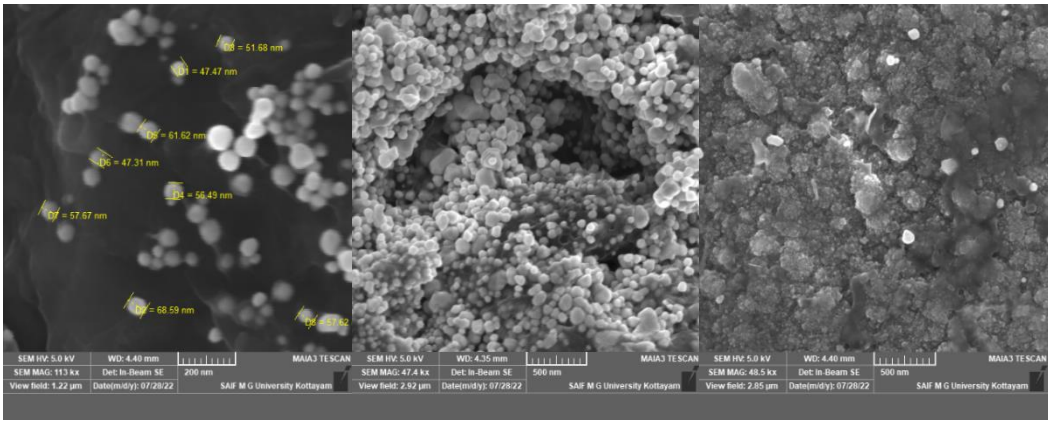

Figure 4.7.3.b: FE-SEM images of rGO/Ag nanoparticles

The Ag nano particles are uniformly distributed on the surface of GO sheet with the average size of 50 ± 5 nm [12].

4.7.4 HRTEM analysis of rGO/Ag nano composite

The structure and morphology of as prepared rGO/Ag were examined by High resolution Transmission Electron Microscope (HRTEM). Figure 4.7.4 depicts the TEM images of reduced Graphene oxide/ silver nano particles.

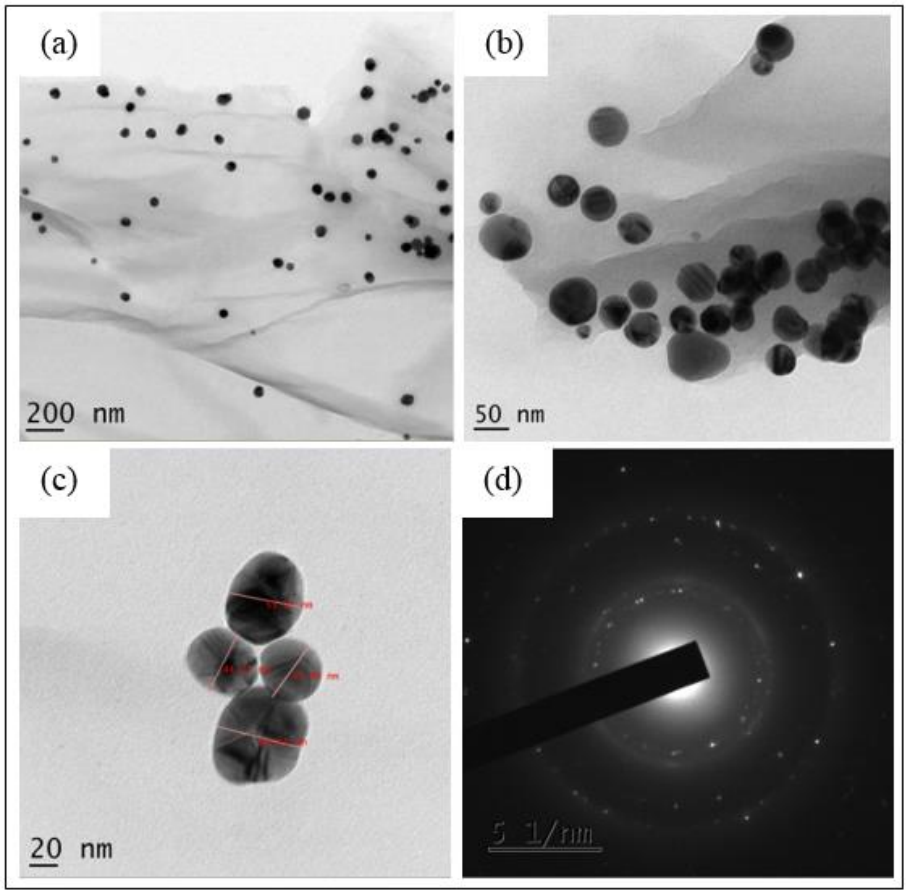

Figure 4.7.4: TEM images of rGO/Ag nano particles in (a),(b) and (c); (d): SAED pattern of rGO/Ag

From the TEM image 4.7.4 (a), it is clear that the graphene sheets are homogeneously exfoliated. The Ag nano spheres are arranged uniformly between the layers of graphene. The evenly distributed Ag nano particles without much aggregation, indicates that GO can act as a strong platform for the growth of silver nano particles [13]. Figure 4.7.4 (c) displays that the Ag nano spheres of diameter ~ 50 nm are dispersed uniformly over the surface of the graphene oxide sheets. The image in figure 4.7.4 (d) indicates the corresponding SAED pattern of Ag nano sphere, which gives an idea about its crystalline nature.

4.7.5 Raman analysis of rGO/Ag nano composites

The Raman peak shown in Fig. 4.7.5 confirms the integration of silver nanoparticles on the surface of graphene oxide sheets.

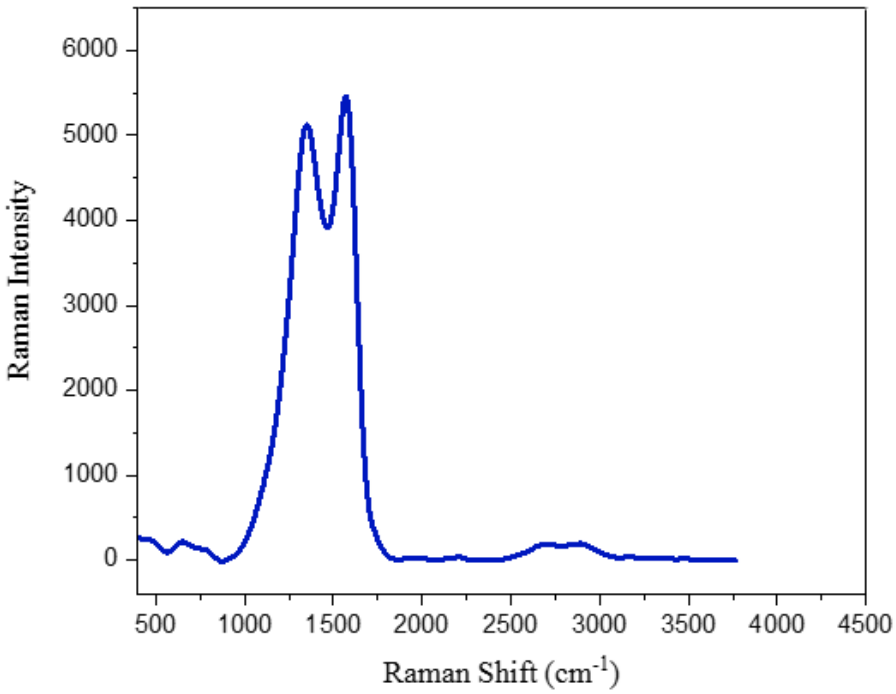

Figure 4.7.5: Raman spectra corresponding to rGO/Ag nano particles

The GO/Ag was characterized by two bands. The D-band at 1345.7 cm^{-1} and G band at 1586.2 cm^{-1}. Here the D band is due to lattice imperfections in at the grain boundary and G band is the characteristic peak due to the E_{2g1} [11]. The 2D peak at 2672.48 cm^{-1} is due to a double resonance intervalley Raman scattering process for graphene transferred on Ag nano particles [14-18]. Here the I_D/I_G ratio is calculated as 1.08 [16].

REFERENCE

1. Paulchamy, Balaiah, G. Arthi, and B. D. Lignesh. "A simple approach to stepwise synthesis of graphene oxide nanomaterial." *J Nanomed Nanotechnol* 6, no. 1 (2015): 1.

2. Luu, Quocanh N., Joshua M. Doorn, Mary T. Berry, Chaoyang Jiang, Cuikun Lin, and P. Stanley May. "Preparation and optical properties of silver nanowires and silver-nanowire thin films." *Journal of colloid and interface science* 356, no. 1 (2011): 151-158.

3. Naeem, Hina, Muhammad Ajmal, Raheela Beenish Qureshi, Sedra Tul Muntha, Muhammad Farooq, and Muhammad Siddiq. "Facile synthesis of graphene oxide–silver nanocomposite for decontamination of water from multiple pollutants by adsorption, catalysis and antibacterial activity." *Journal of environmental management* 230 (2019): 199-211.

4. Kumari, Sujata, Pratibha Sharma, Sunny Yadav, Jitender Kumar, Ankush Vij, Pooja Rawat, Shalendra Kumar et al. "A novel synthesis of the graphene oxide-silver (GO-Ag) nanocomposite for unique physiochemical applications." *ACS omega* 5, no. 10 (2020): 5041-5047.

5. Jose, Priya Parvathi Ameena, M. S. Kala, Nandakumar Kalarikkal, and Sabu Thomas. "Reduced graphene oxide produced by chemical and hydrothermal methods." *Materials Today: Proceedings* 5, no. 8 (2018): 16306-16312.

6. Siburian, Rikson, Hotmaulina Sihotang, S. Lumban Raja, M. Supeno, and Crystina Simanjuntak. "New route to synthesize of graphene nano sheets." *Oriental Journal of Chemistry* 34, no. 1 (2018): 182.

7. Ameer, Shahid, and Iftikhar Hussain Gul. "Influence of reduced graphene oxide on effective absorption bandwidth shift of hybrid absorbers." *PLoS One* 11, no. 6 (2016): e0153544.

8. Gao, Xingfa, Joonkyung Jang, and Shigeru Nagase. "Hydrazine and thermal reduction of graphene oxide: reaction mechanisms, product structures, and reaction design." *The Journal of Physical Chemistry C* 114, no. 2 (2010): 832-842.

9. Hsiao, Min-Chien, Shu-Hang Liao, Ming-Yu Yen, Po-I. Liu, Nen-Wen Pu, Chung-An Wang, and Chen-Chi M. Ma. "Preparation of covalently functionalized graphene using residual oxygen-containing functional groups." *ACS applied materials & interfaces* 2, no. 11 (2010): 3092-3099.

10. Sahu, Sumit Ranjan, Mayanglambam Manolata Devi, Puspal Mukherjee, Pratik Sen, and Krishanu Biswas. "Optical property characterization of novel graphene-X (X= Ag, Au and Cu) nanoparticle hybrids." *Journal of Nanomaterials* 2013 (2013).

11. Jose P, Kala M, “Silver attached reduced graphene oxide as sunlight induced photocatalyst

for dye degradation", International conference, MEETCON'17

12. Khorrami, Sadegh, Zahra Abdollahi, Ghazaleh Eshaghi, Arezoo Khosravi, Elham Bidram, and Ali Zarrabi. "An improved method for fabrication of Ag-GO nanocomposite with controlled anti-cancer and anti-bacterial behavior; a comparative study." *Scientific Reports* 9, no. 1 (2019): 1-10.

13. Li, Leilei, Lulu Fan, Min Sun, Huamin Qiu, Xiangjun Li, Huimin Duan, and Chuannan Luo. "Adsorbent for chromium removal based on graphene oxide functionalized with magnetic cyclodextrin–chitosan." *Colloids and Surfaces B: Biointerfaces* 107 (2013): 76-83.

14. Malard, L. M., Marcos Assunção Pimenta, Gene Dresselhaus, and M. S. Dresselhaus. "Raman spectroscopy in graphene." *Physics reports* 473, no. 5-6 (2009): 51-87.

15. Ni, Zhenhua, Yingying Wang, Ting Yu, and Zexiang Shen. "Raman spectroscopy and imaging of graphene." *Nano Research* 1, no. 4 (2008): 273-291.

16. Sheng, Zhen-Huan, Lin Shao, Jing-Jing Chen, Wen-Jing Bao, Feng-Bin Wang, and Xing-Hua Xia. "Catalyst-free synthesis of nitrogen-doped graphene via thermal annealing graphite oxide with melamine and its excellent electrocatalysis." *ACS nano* 5, no. 6 (2011): 4350-4358.

17. Nair, Anju K., M. S. Kala, Sabu Thomas, and Nandakumar Kalarikkal. "Reduced graphene oxide wrapped Ag nanostructures for enhanced SERS activity." In *AIP Conference Proceedings*, vol. 1942, no. 1, p. 050094. AIP Publishing LLC, 2018.

18. Cozzoli, P. Davide, Roberto Comparelli, Elisabetta Fanizza, M. Lucia Curri, Angela Agostiano, and Daniele Laub. "Photocatalytic synthesis of silver nanoparticles stabilized by TiO2 nanorods: A semiconductor/metal nanocomposite in homogeneous nonpolar solution." *Journal of the American Chemical Society* 126, no. 12 (2004): 3868-3879.

CHAPTER 5

APPLICATIONS

Surface enhanced Raman scattering technique (SERS) has reported some promising applications in fields like chemical detection, environmental monitoring, food safety and bio-medical spheres. It can provide a finger print like information of the target molecule, which makes it an appropriate tool for on-site testing of harmful chemicals [1-4].

5.1 Dye detection

Dyes are chemical compound that are mainly used for imparting colours onto textiles like silk, jute, cotton, wool and other articles like, leather, cosmetics, plastic utensils, paper, food, etc. [5-7] The most commonly used dyes are methylene blue, crystal violet (CV), malachite green (MG), congo red (MB), rhodamine B, rhodamine 6G (R6G), etc. Their cost and ease of use make them an attractive factor in food colouring as well [8]. Most of the above mentioned dyes are soluble in aqueous as well as in organic solvents. Due to their carcinogenic nature, it causes several serious health issues such as irritation to the skin, eyes, and respiratory system [9, 10]. Therefore, it is high time to track their presence in materials even at the very low concentration.

Crystal violet is a chemical compound with the molecular formula $C_{25}N_3H_{30}Cl$. It is used on large scale as an anti-fungual agent especially in aquaculture [10]. It is a drug used against different fish diseases. However, due to their harmful effects on human health, these are banned in many counties including USA, Japan, etc. [10,11]. But in order to have export quality products, the illegal use of these kind of chemical dyes are still in effect. In order to ensure safety towards such aqua products, effective detection measurements should be taken.

Among the various detection methods like high performance liquid chromatorgraphy, fluorimety, electro chemical detection, etc. the surface enhanced Raman spectroscopic method is the most effective. rGO/Ag SERS substrate can enhance their activity towards the targeted molecule, which makes them suitable for on-site dye detection. [1-4].

5.1.1 rGO/Ag substrate as a Dye detector

Figure 5.1.1.a, shows the normal Raman spectrum of chemical dye crystal violet adsorbed on a glass slide without the SERS substrate.

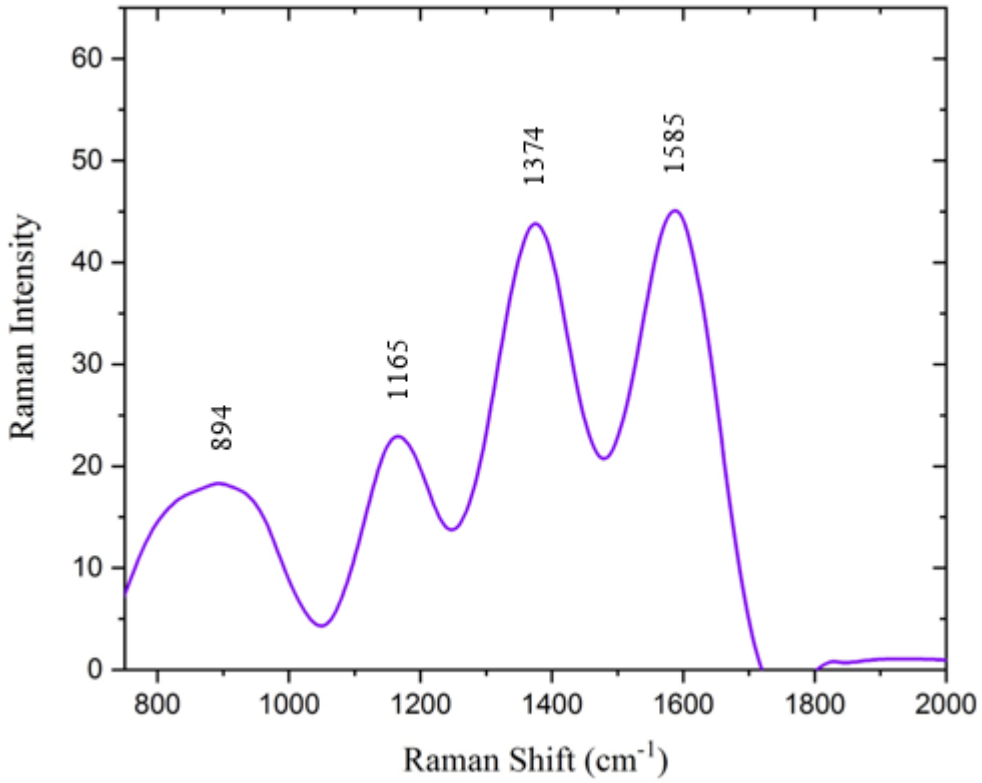

Figure 5.1.1.a: Raman spectrum of crystal violet

In the Raman spectrum of crystal violet bulk, the band observed at 894 cm^{-1} is caused by C-H out of plane bending mode, whereas the medium band at 1165 cm^{-1} is attributed to the C-H in-plane bending mode [12][13]. The overlapped vibrational stretching of $CC_{centre}C$ and stretching vibration of nitrogen and phenyl ring attributes to the band at 1374 cm^{-1} [12]. The prominent band at 1585 cm^{-1} is due to in-plane aromatic C-C stretching vibration [13].

In order to study the enhancement factor, the efficiency in determining crystal violet in rGO/Ag SERS substrate is to be compared with those in GO as well as Ag nano particles. The corresponding results are shown in figure 5.1.1.b.

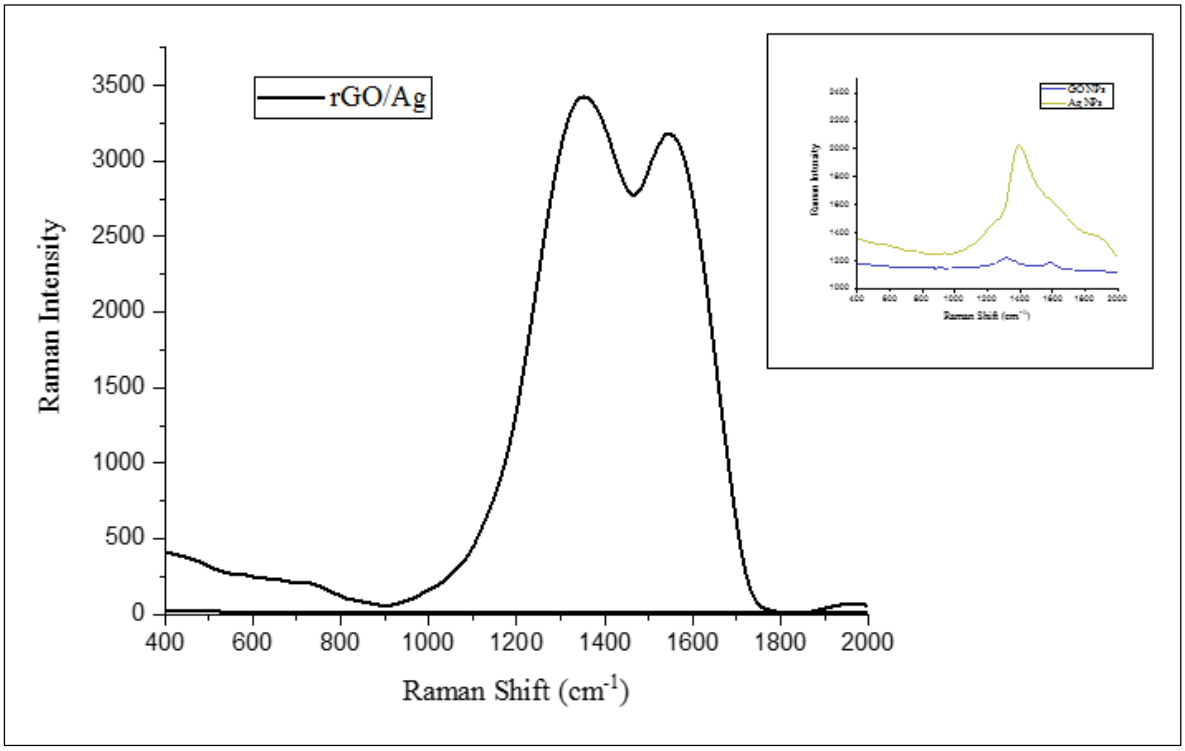

Figure 5.1.1.b: SERS spectra of crystal violet at 10^{-8} M concentration

SERS spectum of crystal violet with the concentration of 10^{-8} M obtained from the rGO/Ag nano composite substrate is given in Figure 5.1.1.b The inset shows the corresponding spectra obtained from GO and Ag nano particles respectively. Comparing the peaks, we can conclude that the sensing property on rGO/Ag nano composite SERS substrate is more enhanced than that on the GO or Ag nano particles substrates. This alludes to the charge transfer mechanism between the adsorbate and SERS substrate involved in the process [18].

Later, the detection of crystal violet with concentration ranging from 10^{-11} M to 10^{-2} M was examined on rGO/Ag nano composite SERS substrate. The results obtained have been depicted in Figure 5.1.1.c.

The three major peaks with small deviations at 880 cm^{-1} is attributed to $\sigma(CC_{center}C)$, while those at 1357 cm^{-1} is attributed to $\sigma(CCC)_{rings}$, σ_{as} $(CC_{center}C)$ & $\sigma(CH)$. The peak at 1553 cm^{-1} is attributed to σ_{as} (C-C) or $\upsilon(C_{ring}\text{-}N)$.

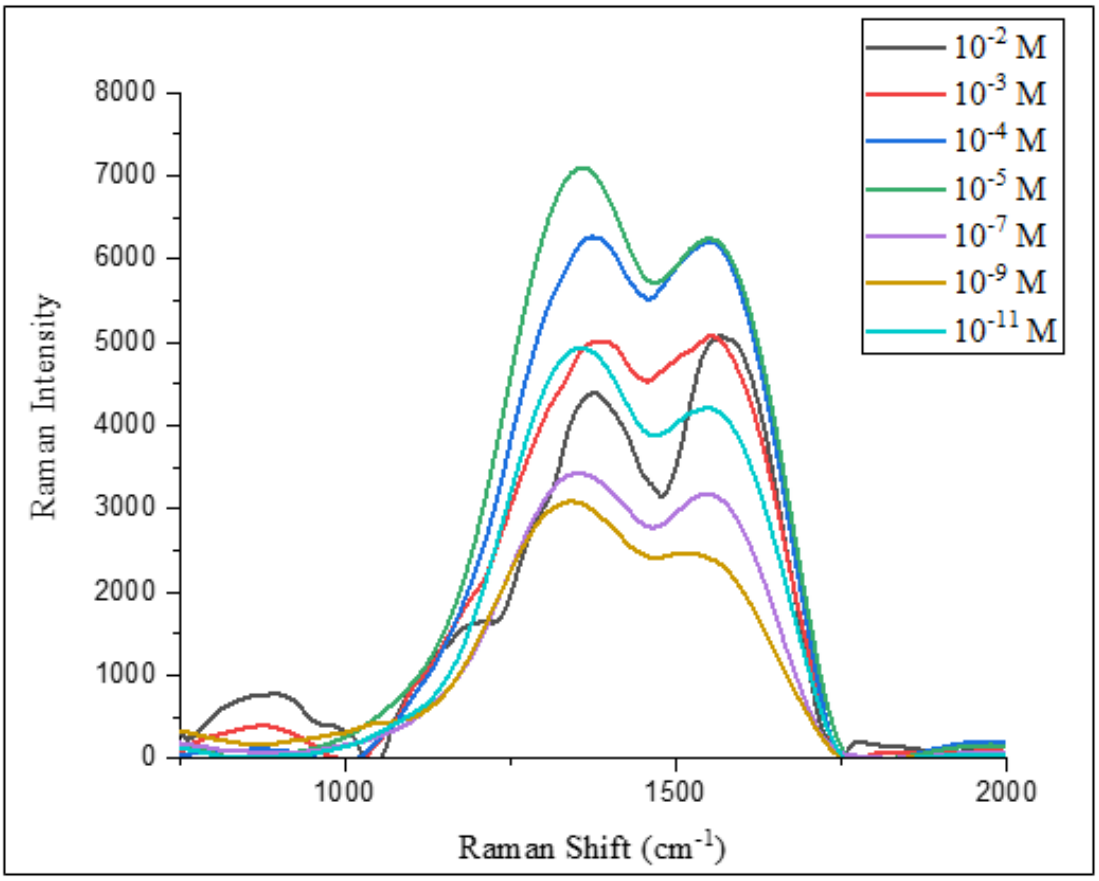

Figure 5.1.1.c: SERS spectra of crystal violet with different concentrations adsorbed on rGO/Ag substrate

Here, as the detection limit reaches 10^{-11} M, it ensures the high sensitivity of SERS substrate for crystal violet.

5.2 Pesticide sensing

With the advent of commercialization, the practise of farming and cultivation has declined. Those engaged in agriculture now focus on yielding more quantity than better quality products. Thus pesticides including insecticides, fungicides, and herbicides became important players in agriculture. Nearly 1000 variety of pesticides are used all over the world. The most commonly used pesticides are chloropyrifos, thiram, ethoprophos, parathion-ethyl, methamidophos, thiabendazole, pATP, endosulfan etc. The over dosage or use of multiple pesticides are not only hazardous to human beings but also to the surrounding ecosystem [16][17]. The non- standard use of these chemicals should be detected and controlled with an effective technique.

Here, the pesticide thiram with molecular formula $C_6H_{12}N_2S_4$ was used for analysis. It is also called as thiuram disulphide. It is commonly used as a fungicide and an ectoparasiticide. It is highly toxic and can cause serious health issues such as nausea, diarrhoea, gastrointestinal complaints etc. [21] The effective detection of the pesticide thiram was done using the rGO/Ag SERS substrate prepared.

5.2.1 rGO/Ag substrate as a Pesticide Sensor

From Figure 5.2.1.a, the sensing ability of SERS substrate for the pesticide – 'thiram' can be studied.

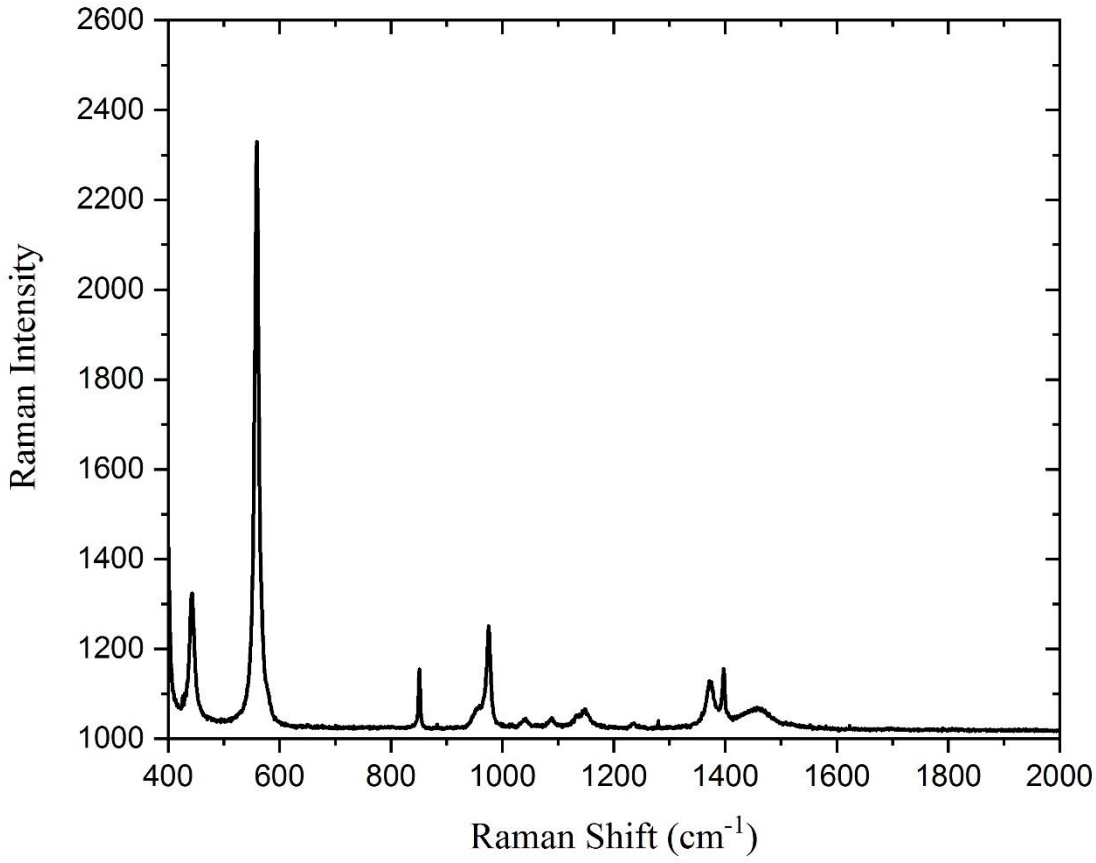

Figure 5.2.1.a: Raman spectra of Thiram

The band at 443 cm^{-1} corresponds to $\sigma(CH_3NC)$ or $\upsilon(C=S)$ and the prominent band at 560 cm^{-1} is attributed to $\upsilon(S-S)$. The other bands observed at 852 cm^{-1} and 976 cm^{-1} are attributed to $\upsilon(CH_3N)$.While the peak at 1147 cm^{-1} corresponds to $\rho(CH_3)$ or $\upsilon(C-N)$. And the adjacent bands at 1370 cm^{-1} and 1395 cm^{-1} are attributed to $\sigma_s(CH_3)$ or $\upsilon(C-N)$

and $\sigma_{as}(CH_3)$ repectively. The $\upsilon(C-N)$, $\sigma(CH_3)$ or $\rho(CH_3)$ attribute the small peak at 1464 cm^{-1} [14][15].

Figure 5.2.1.b indicates the sensing capacity of rGO/Ag SERS substrate with just the GO and Ag nano particles towards the pesticide thiram. The peaks at 586 cm^{-1}, 1320 $cm^{-1}$and 1589 cm^{-1} are recorded at 10^{-8} M concentration of Thiram. By comparing the spectra, we can conclude that the rGO/Ag nano composite SERS substrate shows an enhanced sensing property.

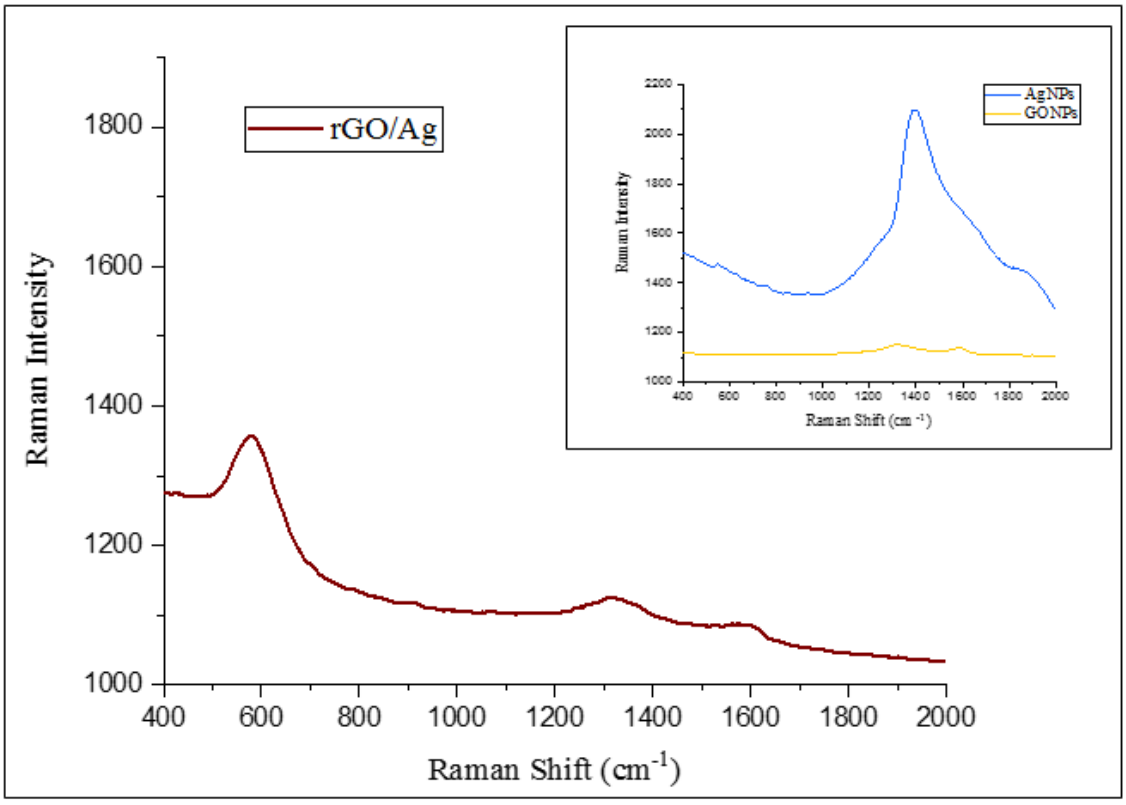

Figure 5.2.1.b: Raman spectra of thiram at 10^{-8} M concentration

The SERS spectra of Thiram with different concentrations ranging from 10^{-9} M to 10^{-5} M on rGO/Ag SERS substrate is shown in the figure 5.2.1.c.

Thus, the results indicates that the prepared substrate has good enhancement effect on sensing of the pesticide thiram even at a low limit of detection, that is at 10^{-9} M.

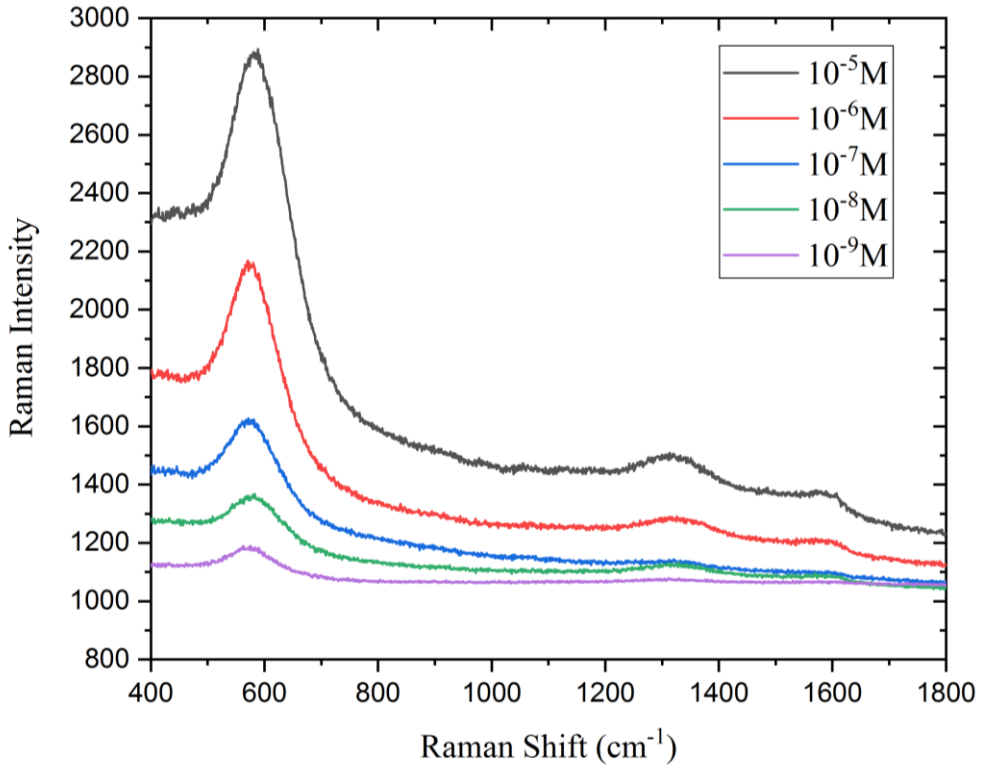

Figure 5.2.1.c: SERS spectra of Thiram with different concentrations adsorbed on rGO/Ag substrate

Measurements were taken at 8 random points to check the reproducibility and stability of the substrate. Figure 5.2.1.d illustrates the corresponding graphs. By taking into consideration the similarity in all cases, uniformity and reproducibility of the substrate can be vouched for.

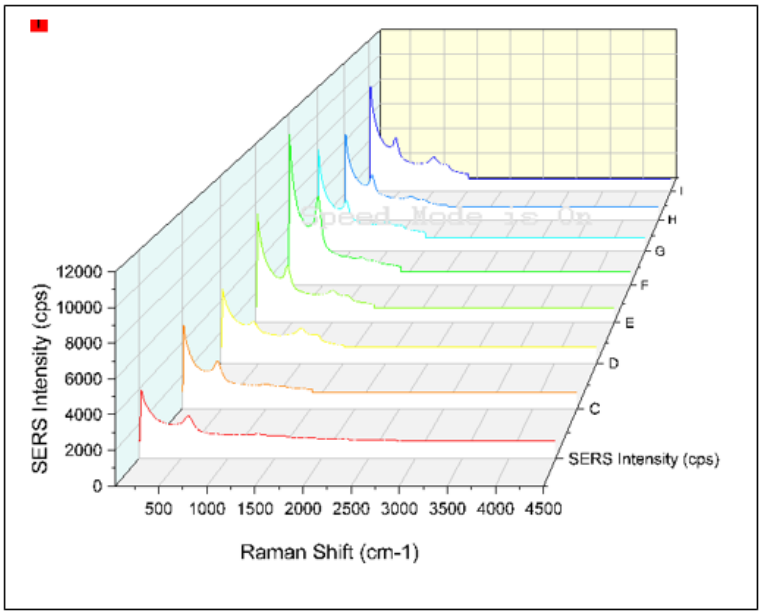

Figure 5.2.1.d: SERS spectra of Thiram on rGO/Ag at different spots (concentration 10^{-5} M)

5.3 Antimicrobial study

Trillion microbes are present in and on our body. They are the basic factors that drive our health by maintaining proper digestion, protecting from infections, regulating respiration, etc. These microbes can be generally categorized as bacteria, fungi, protozoa, archaea and algae. Most of these microbes are not harmful. While Saccharomyces cerevisia, Aspergillus oryzae, L. plantarum, etc. are considerd as useful microorganisms, those like Escherichia coli (E. coli), Staphylococcus aureus, Mycobacterium tuberculosis, etc. are harmful microorganisms that can damage the human body. Some of these microbes can even destroy food crops and clothing.

Now, the complete removal of these microbes by inhibiting their cell replication is of high importance. The efficiency of silver in deactivating the harmful microorganisms are well known. Therefore, in order to study the antimicrobial activity of as prepared rGO/Ag nano composite, it was assessed against two bacterial strains: E. coli and S. aureus.

5.3.1 rGO/Ag nano composite as an Antibacterial agent

In order to understand the antibacterial activity of GO/Ag nano composite, two bacterial strains (Gram-negative bacterium, E. coli and the Gram-positive bacterium, S. aureus) were used.

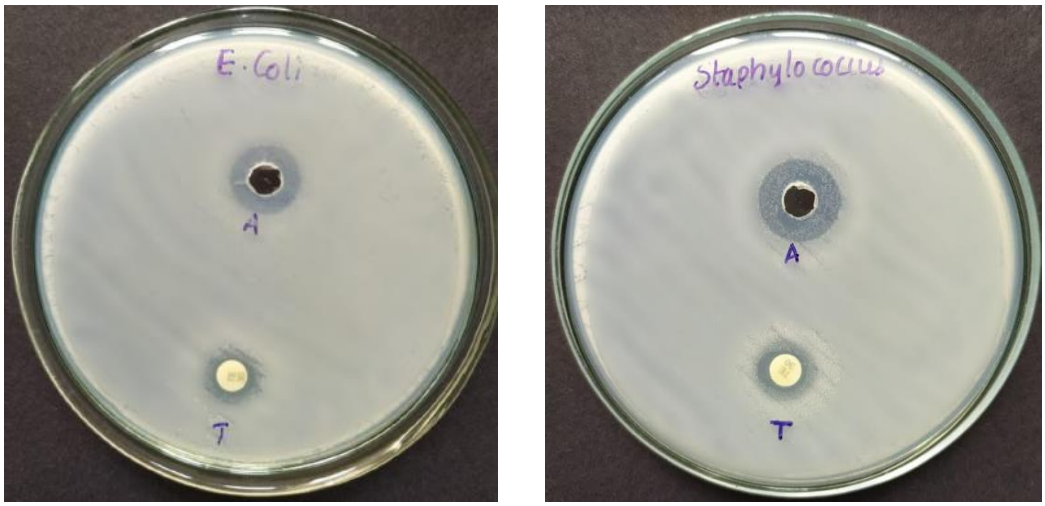

Figure 5.3.1: Antibacterial activity rGO/Ag nano composite on (a) E. coli (b) Staphylococcus

Here the method followed consists of measuring the zone inhibited in a disk diffusion test against E.coli and staphylococcus. The control used here was Tetracycline (TE) 30 mcg susceptibility Test discs, which is denoted as T in the figure 5.3.1. The zone inhibited against

E.coli for 0.01g/ml of rGO/Ag nano composite was measured as 12 mm, while the zone inhibition caused by the control in E.coli came upto 9 mm. Similar significant zone inhibition was also noted against S. aureus and it was found to be at 6 mm for the same quantity of GO/Ag nano composite. The zone inhibition made by control in S. aureus was 5 mm. The results from zone inhibition study confirmed the remarkable performance of the nanocomposite in destroying harmful pathogens [22]. These results are consistent with previous observations made by Bao et al., 2011; Ma et al., 2011 [23].

REFERENCE

1. Phung, Viet-Duc, Won-Sik Jung, Jong-Hoon Kim, and Sang-Wha Lee. "Gold nanostructures electrodeposited on graphene oxide-modified indium tin oxide glass as a surface-enhanced Raman scattering-active substrate for ultrasensitive detection of dopamine neurotransmitter." *Japanese Journal of Applied Physics* 57, no. 8S2 (2018): 08PF02.

2. Phung, Viet-Duc, Won-Sik Jung, Thuy-An Nguyen, Jong-Hoon Kim, and Sang-Wha Lee. "Reliable and quantitative SERS detection of dopamine levels in human blood plasma using a plasmonic Au/Ag nanocluster substrate." *Nanoscale* 10, no. 47 (2018): 22493-22503.

3. Zhang, Wending, Cheng Li, Kun Gao, Fanfan Lu, Min Liu, Xin Li, Lu Zhang et al. "Surface-enhanced Raman spectroscopy with Au-nanoparticle substrate fabricated by using femtosecond pulse." *Nanotechnology* 29, no. 20 (2018): 205301.

4. Li, Zi Hao, Jia Hao Bai, Xin Zhang, Jia Meng Lv, Cheng Shan Fan, Yong Mei Zhao, Zheng Long Wu, and Hai Jun Xu. "Facile synthesis of Au nanoparticle-coated Fe3O4 magnetic composite nanospheres and their application in SERS detection of malachite green." *Spectrochimica Acta Part A: Molecular and Biomolecular Spectroscopy* 241 (2020): 118532.

5. Chiang, Tsung-Ling, Yu-Chen Wang, and Wang-Hsien Ding. "Trace determination of rhodamine B and rhodamine 6G dyes in aqueous samples by solid-phase extraction and high-performance liquid chromatography coupled with fluorescence detection." *Journal of the chinese chemical society* 59, no. 4 (2012): 515-519.

6. He, Quanguo, Jun Liu, Yonghui Xia, Du Tuo, Peihong Deng, Yaling Tian, Yiyong Wu, Guangli Li, and Dongchu Chen. "Rapid and sensitive voltammetric detection of rhodamine B in chili-containing foodstuffs using MnO2 nanorods/electro-reduced graphene oxide composite." *Journal of The Electrochemical Society* 166, no. 10 (2019): B805.

7. Baldev, E., D. MubarakAli, A. Ilavarasi, D. Pandiaraj, KA Sheik Syed Ishack, and N. Thajuddin. "Degradation of synthetic dye, Rhodamine B to environmentally non-toxic products using microalgae." *Colloids and Surfaces B: Biointerfaces* 105 (2013): 207-214.

8. X. Zhu, G. Wu, C. Wang, D. Zhang, X. Yuan, A miniature and low-cost electrochemical system for sensitive determination of rhodamine B, Measurement 120 (2018) 206–212

9. Lu, X. W., Z. Dang, and C. Yang. "Preliminary investigation of chloramphenicol in fish, water and sediment from freshwater aquaculture pond." *International Journal of Environmental Science & Technology* 6, no. 4 (2009): 597-604.

10. Andersen, Wendy C., Sherri B. Turnipseed, Christine M. Karbiwnyk, Rebecca H. Lee, Susan B. Clark, W. Douglas Rowe, Mark R. Madson, and Keith E. Miller. "Quantitative and confirmatory analyses of crystal violet (gentian violet) and brilliant green in fish." *US Food and Drug Administration, Laboratory Information Bulletin* 4395 (2007).

11. Shi, Xizhi, Aibo Wu, Sulian Zheng, Rongxiu Li, and Dabing Zhang. "Molecularly imprinted polymer microspheres for solid-phase extraction of chloramphenicol residues in foods." *Journal of Chromatography B* 850, no. 1-2 (2007): 24-30.

12. Strehle, Katrin R., Dana Cialla, Petra Rösch, Thomas Henkel, Michael Köhler, and Jürgen Popp. "A reproducible surface-enhanced Raman spectroscopy approach. Online SERS measurements in a segmented microfluidic system." *Analytical Chemistry* 79, no. 4 (2007): 1542-1547.

13. Volný, Michael, Atanu Sengupta, C. Brant Wilson, Brian D. Swanson, E. James Davis, and František Tureček. "Surface-enhanced Raman spectroscopy of soft-landed polyatomic ions and molecules." *Analytical chemistry* 79, no. 12 (2007): 4543-4551.

14. Kang, Jae-Soo, Seon-Yeong Hwang, Chul-Jae Lee, and Mu-Sang Lee. "SERS of dithiocarbamate pesticides adsorbed on silver surface; thiram." *Bulletin of the Korean Chemical Society* 23, no. 11 (2002): 1604-1610.

15. Liu, Bianhua, Guangmei Han, Zhongping Zhang, Renyong Liu, Changlong Jiang, Suhua Wang, and Ming-Yong Han. "Shell thickness-dependent Raman enhancement for rapid identification and detection of pesticide residues at fruit peels." *Analytical chemistry* 84, no. 1 (2012): 255-261.

16. Li, Yongyu, Yunyun Sun, Yankun Peng, Sagar Dhakal, Kuanglin Chao, and Qiaoqiao Liu. "Rapid detection of pesticide residue in apple based on Raman spectroscopy." In *Sensing for agriculture and food quality and safety IV*, vol. 8369, pp. 128-133. SPIE, 2012.

17. Chai, Lian-Kuet, and Fatimah Elie. "A rapid multi-residue method for pesticide residues determination in white and black pepper (Piper nigrum L.)." *Food Control* 32, no. 1 (2013): 322-326.

18. Jose, Priya Parvathi Ameena, M. S. Kala, Alphonsa Vijaya Joseph, Nandakumar Kalarikkal, and Sabu Thomas. "Reduced graphene oxide/silver nanohybrid as a multifunctional material for antibacterial, anticancer, and SERS applications." *Applied Physics A* 126, no. 1 (2020): 1-16.

19. Tsochatzis, Emmanouil D., Urania Menkissoglu-Spiroudi, Dimitrios G. Karpouzas, and Roxani Tzimou-Tsitouridou. "A multi-residue method for pesticide residue analysis in rice grains using matrix solid-phase dispersion extraction and high-performance liquid chromatography–diode array detection." *Analytical and Bioanalytical Chemistry* 397, no. 6 (2010): 2181-2190.

20. Fernández, M., Y. Picó, and J. Manes. "Determination of carbamate residues in fruits and vegetables by matrix solid-phase dispersion and liquid chromatography–mass spectrometry." *Journal of Chromatography A* 871, no. 1-2 (2000): 43-56.

21. Hayes, W.J. and E.R. Laws, ed. (1990). *Handbook of Pesticide Toxicology*. Vol. 3, Classes of Pesticides. NY: Academic Press, Inc.

22. Naeem, Hina, Muhammad Ajmal, Raheela Beenish Qureshi, Sedra Tul Muntha, Muhammad Farooq, and Muhammad Siddiq. "Facile synthesis of graphene oxide–silver nanocomposite for decontamination of water from multiple pollutants by adsorption, catalysis and antibacterial activity." *Journal of environmental management* 230 (2019): 199-211.

23. Bao, Qi, Dun Zhang, and Peng Qi. "Synthesis and characterization of silver nanoparticle and graphene oxide nanosheet composites as a bactericidal agent for water disinfection." *Journal of colloid and interface science* 360, no. 2 (2011): 463-470.

24. Zhang, Li, Bin Wang, Guang Zhu, and Xia Zhou. "Synthesis of silver nanowires as a SERS substrate for the detection of pesticide thiram." *Spectrochimica Acta Part A: Molecular and Biomolecular Spectroscopy* 133 (2014): 411-416.

25. Sahu, Sumit Ranjan, Mayanglambam Manolata Devi, Puspal Mukherjee, Pratik Sen, and Krishanu Biswas. "Optical property characterization of novel graphene-X (X= Ag, Au and Cu) nanoparticle hybrids." *Journal of Nanomaterials* 2013 (2013).

CHAPTER 6

CONCLUSION

In conclusion, we have designed an environment friendly substrate that aids in the easier detection of chemicals by employing a low cost solvothermal method. The fabricated rGO/Ag nano composites can act as an excellent SERS (Surface Enhanced Raman Spectroscopy) substrate for the detection of certain chemicals at subnanomolar levels. The detection of one of the most harmful and commonly used water pollutant – crystal violet, a chemical dye was done successfully. Traces of crystal violet at various concentrations ranging from 10 -2 M to 10 -11 M gave reliable peaks on SERS substrate. This result backs the claim that the substrate can be effectively employed in the detection of crystal violet at concentrations as low as 10 -11 M. The sensing capability of rGO/Ag against the pesticide thiram in iso propyl alcohol was also demonstrated. The study also noted that in the presence of the rGO/Ag SERS substrate, thiram molecules displayed an enhanced peak even at a low concentration of 10 -9 M. Hence it is safe to conclude that this could be a promising technique for sensing the pesticide, Thiram in more practical situations. In addition, the antibacterial activity of rGO/Ag nano composite was tested against two bacteria: Gram-negative bacterium, E. coli and the Gram-positive bacterium, S. aureus. The observations made indicate a good scope for their applications in the bio-medical field.